Ruthenium(II) and Osmium(II) Bis(terpyridine) Complexes in Covalently-Linked Multicomponent Systems: Synthesis, Electrochemical Behavior, Absorption Spectra, and Photochemical and Photophysical Properties

Jean-Pierre Sauvage,* Jean-Paul Collin, Jean-Claude Chambron, Stephane Guillerez, and Christophe Coudret

Laboratoire de Chimie Organo-minérale, Institut de Chimie, Université de Strasbourg, 67008 Strasbourg, France

Vincenzo Balzani,* Francesco Barigelletti,* Luisa De Cola, and Lucia Flamigni

Dipartimento di Chimica "G. Ciamician", Università di Bologna, and Istituto FRAE-CNR, 40126 Bologna, Italy

Received December 13, 1993 (Revised Manuscript Received March 22, 1994)

Contents

1. Introduction

A photon is at the same time a quantum of energy and a bit of information. The interaction of light with "matter" can therefore be used for energy or information purposes. The results that can be obtained depend on the degree of organization of the receiving "matter".

The simplest form of organization is that of a small number of atoms in a molecule. The interaction of photons with molecules can cause *simple acts*, such as a change in the molecular structure (isomerization), which can be exploited, in principle, for both energy and information purposes. For example, solar energy can be converted into (and stored as) chemical energy by transforming norbornadiene into its higher energy quadricyclane isomer,[1] and laser beams can write (and also erase) bits of information on spiropyran photochromic molecules.[2]

A higher level of organization is the assembly of a discrete number of molecular components to yield supramolecular species.[3-10] Supramolecular organization can be attained by intermolecular forces of various type (Coulombic interactions, hydrogen bonds, etc.) or by linking together molecular components by covalent bonds.[11] By these routes it is possible to put together prefabricated molecular components that carry the desired light-related properties: absorption spectrum, excited-state lifetime, luminescence spectrum, excited-state redox properties, etc. This allows us to design structurally organized and functionally integrated systems[5] (photochemical molecular devices, PMDs)[7,13] capable of elaborating the energy and information input of photons to perform *complex functions* (light harvesting,[14-17] conversion of light into chemical[17-19] or electrical energy,[20] collection of information in a molecular shift register,[21] etc.).[7]

2. Natural vs Artificial Photochemical Molecular Devices

PMDs are present, of course, in nature where they perform functions essential to life such as photosyn-

0009-2665/94/0794-0993$14.00/0

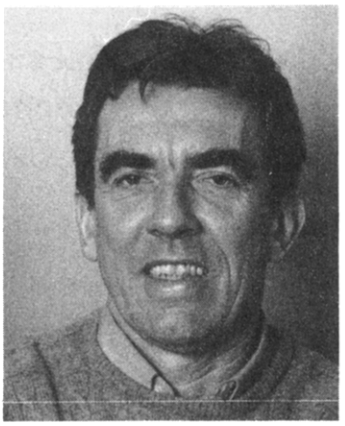

Jean-Pierre Sauvage was born in 1944 in Paris. After studying at Strasbourg University, he did his Ph.D. with J.-M. Lehn on cryptates and spent some time as a post-doc with M. L. M. Green at Oxford (U.K.). He is now a research director (CNRS) at the Faculty of Chemistry. His main scientific interests range from chemical topology (catenanes and knots) to models of the photosynthetic reaction center and one-dimensional multicomponent transition complexes.

Jean-Paul Collin was born in 1945 in Metz. After his Ph.D. in electrochemistry with Prof. J. P. Schwing at the Louis Pasteur University, Strasbourg, he did postdoctoral work with Prof. J.-M. Lehn on water photolysis. He is now a CNRS research director. He joined Dr. J.-P. Sauvage's group in 1983, and his present research field concerns photoinduced charge separation in multicomponent molecular systems.

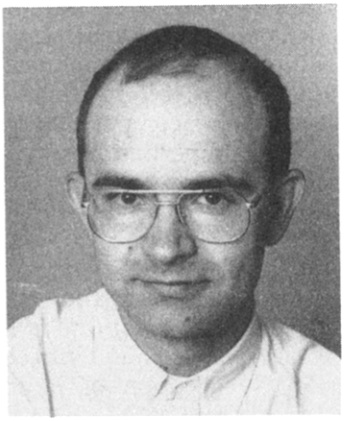

Jean-Claude Chambron was born in Strasbourg in 1959. He did his Ph.D. thesis with Dr. J.-P. Sauvage. Then he spent a postdoctoral year, working with Prof. K. N. Raymond at the University of California (Berkeley). In 1987 he joined J.-P. Sauvage's group as a CNRS researcher. His current research interests are concerned with chemical topology and photoinduced electron transfer.

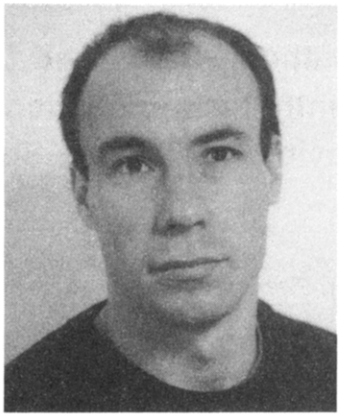

Stéphane Guillerez was born in France in 1963. He received his Ph.D. from the Université Louis Pasteur (Strasbourg) in 1991 working with Dr. J.-P. Sauvage. After one year as a postdoctoral fellow at the University of Sheffield (Prof. J.-F. Stoddart), he joined the Commissariat à l'Energie Atomique. He is now working in the Laboratoire d'Electrochimie Moleculaire (Grenoble) with G. Bidan, on the development of new materials based on electronic conducting polymers.

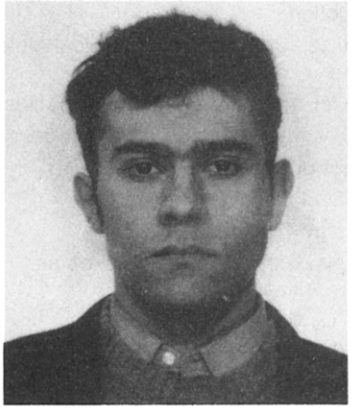

Christophe Coudret was born in Paris in 1966. A former student of the Ecole Normale Supérieure (Paris), he received his "agrégation de chimie" in 1988. He then joined Dr. J.-P. Sauvage's group and obtained his Ph.D. in 1991. After one year as a postdoctoral fellow with Dr. A. Harriman at the Center for Fast Kinetics Research in Austin, TX, he joined Prof. J.-P. Launay's group as a CNRS researcher in Toulouse. His present research field concerns molecular electronics.

thesis and vision. Important progress toward the understanding of such natural PMDs has been made in recent years.[22-29] Examination of natural PMDs shows the fundamental principles that must guide scientists in the design of artificial PMDs.

The conversion of light energy into chemical energy in natural photosynthetic processes is based on two types of PMDs:[22] (1) antenna devices, which are made of hundreds of pigments able to collect solar light and to convey the resulting electronic excitation energy to specific sites (reaction centers), and (2) reaction centers, where the excitation energy is used to perform a charge-separation process which converts electronic energy into redox chemical energy. The determination of the X-ray structures of the reaction centers of the photosynthetic bacteria *Rhodopseudomonas viridis*[24,25,30] and *Rhodobacter sphaeroides*[28] has provided a sound basis for the interpretation of the primary events in the photoinduced charge-separation process. In the reaction center of the *Rps. viridis* the key molecular components

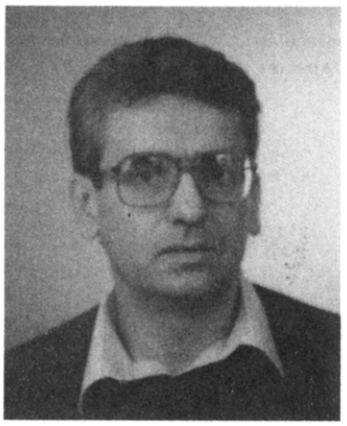

Vincenzo Balzani received his "Laurea" in Chemistry from the University of Bologna in 1960. After a few years as an assistant professor at the University of Ferrara, he joined the Faculty of Science of the University of Bologna in 1969, where he has remained to this day, becoming Professor in 1972. He has served the chemical community as chairman of the European Photochemistry Association and of several meetings, including the XII IUPAC Symposium on Photochemistry and the NATO Science Forum on Supramolecular Chemistry. His research interests include photochemistry, photophysics, electronic spectroscopy, electrochemistry, thermal and photoinduced electron transfer reactions, chemiluminescence, supramolecular chemistry, and molecular devices.

Francesco Barigelletti was born in 1944. He got is "Laurea" in Chemistry in 1971. After a postdoctoral fellowship and a leave for the draft with Army, he joined National Research Council of Italy in 1973. His interests have been in the photochemistry and photophysics of molecular and supramolecular systems for light energy conversion.

Luisa De Cola was born in 1960 in Messina. She studied chemistry at Messina University and then she was a postdoctoral fellow (1984–1985) with Prof. L. M. Vallarino at Virginia Commonwealth University. Since 1986 she has joined Prof. V. Balzani's group in Bologna. In 1990 she was appointed as "researcher" at the University of Bologna. Her research interests include photophysics and photochemistry of coordination compounds and energy and electron transfer in polynuclear complexes.

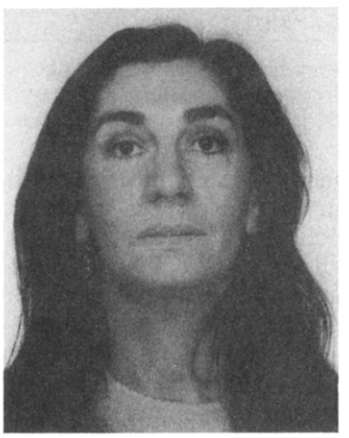

Lucia Flamigni was born in 1949. She obtained her "Laurea" in Chemistry in 1973 at the University of Bologna. She had postdoctoral experiences at the Chemistry Department of the University of Manchester and at C.F.K.R., University of Texas at Austin. She has been researcher at F.R.A.E. Institute since 1982. Her current interests include photoreactivity of dyes in organized media and photoinduced energy and electron transfer in molecular assemblies containing ruthenium and osmium centers.

(Figure 1) are the bacteriochlorophyll "special pair" (P), a bacteriochlorophyll monomer (BC) and a bacteriopheophytin (BP) (that are present in two structurally equivalent branches), a quinone (Q), and a four-heme *c*-type cytochrome (Cy). These chromophores are held in a fixed geometry by surrounding proteins that span the photosynthetic membrane. Excitation of P is followed by a very fast ($\tau \sim 3$ ps) electron transfer to the BP "primary" acceptor (whether the interposed BC plays the role of mediator in a superexchange mechanism[31] or directly intervenes as an intermediate electron acceptor[32] is still a subject of experimental debate).[33-38] The next step is a fast ($\tau \sim 200$ ps) electron transfer from BP to Q,[39] followed by a slower ($\tau \sim 270$ ns) reduction of the oxidized P by the nearest heme group of Cy.[40] At that stage, transmembrane charge separation has been achieved with a quantum yield approaching unity (of course, only a fraction of the energy of the photon is stored as chemical energy since, as shown in Figure 1, there is a loss of chemical potential as one proceeds down the electron transport chain). The rate constants of the various electron transfer steps involved in the charge separation are summarized in the (approximate) energy level diagram of Figure 1, together with those of the nonoccurring $BP^- \rightarrow P^+$ and $Q^- \rightarrow P^+$ charge recombination steps.[41]

Examination of the antenna and charge-separation devices of natural photosynthesis teaches us an important lesson: valuable photochemical functions such as light energy conversion can only be obtained upon a complex elaboration of the absorbed light energy input in the dimensions of *space*, *energy*, and *time* by means of a suitably organized supramolecular system. Proper organization in the dimensions of space and energy is required to generate vectorial energy or electron migration, and proper organization in time is required to assure a successful competition of forward over back transfer processes, i.e. to obtain efficient processes.

It should be realized, however, that natural systems are extremely complicated, so that any synthetic effort

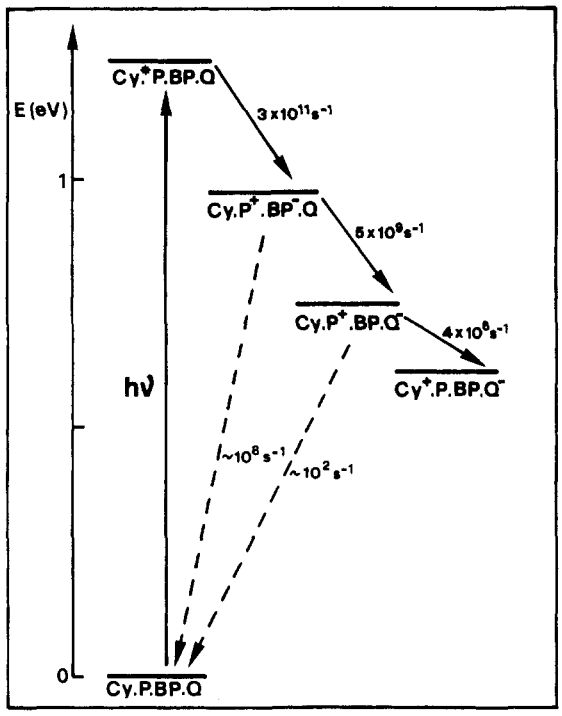

Figure 1. Energy-level diagram and kinetic parameters for the primary processes of bacterial photosynthesis in *Rps. viridis*.

aimed at their exact duplication today would be hopeless. Furthermore, there would be no obvious reason for strictly duplicating natural structures. Such a complexity is related to their living nature, which requires interconnection among many different functions. For example, the production of an apple by nature is the conversion of light energy not simply into chemical energy, but also into genetic informatin, flavor, taste, and a pleasant shape. In artificial photosynthetic systems, we would be fully satisfied to simply convert light energy into a fuel, as it could be done by the generation of hydrogen from the photoinduced water-splitting reaction.

A first obstacle in the construction of artificial PMDs for light energy conversion purposes is the assembly of appropriate molecular components into a suitably organized supramolecular array. In natural systems, supramolecular organization is the "evolutionary" result of a spontaneous self-organization process strictly controlled by intermolecular forces (hydrogen bonds, donor–acceptor interactions, etc.). In spite of the recent progress in molecular recognition and self-assembly processes,[42-53] scientists are not yet capable of designing self-organizing PMDs. In principle, however, chemists are able to design and construct chemically stable and geometrically well-controlled supramolecular structures by linking molecular building blocks *via* covalent bonds.[6-10,13-19,54-59] Most of the artificial PMDs so far investigated for antenna or charge-separation purposes are in fact based on covalently-linked molecular components.[7,10]

To perform a particular function such as, for example, photoinduced charge separation, a PMD needs to be constructed of suitable molecular components, each having a specific role. In principle, we may distinguish three fundamental types of components:[7] (i) active components, which are directly involved in light

Scheme 1

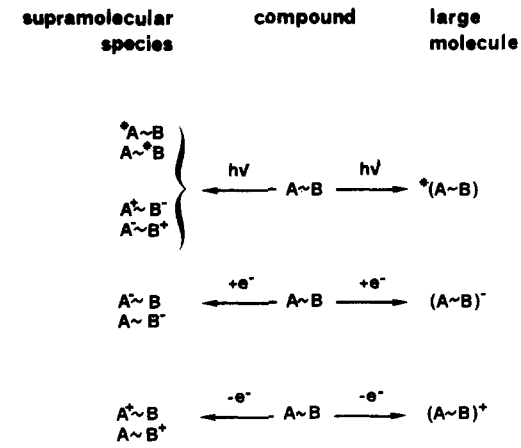

absorption and/or electron/hole migration, (ii) perturbing components, which can be used to modify the properties of active components, and (iii) connecting components, which can be used to link together the active components. It should be pointed out that the connecting components, besides having a *structural* function (i.e., the control of the distance between the active components, the degree of rigidity of the supramolecular structure, etc.) may also have the important role of connecting the active components in an *electronic* sense.

In artificial PMDs, a relatively small variety of active, perturbing, and connecting components has so far been used.[7] Basically, two different approaches have been followed. The first one is "biomimetic", in the sense that the molecular components to be assembled are structurally reminescent of those found in natural systems (porphyrins instead of bacteriochlorophylls, bacteriopheophytins, etc.; quinone and carotenoids as acceptors; etc.). The second strategy deliberately uses totally "abiotic" components, particularly complexes of the second row transition metals and small organic molecules. In this article, we will discuss the advantages and limitations offered by a specific type of active component, the bis(terpyridine)–metal complexes, as photosensitizers.

3. Molecular and Supramolecular Species

Before going on to discuss photoinduced energy- and electron-transfer processes in artificial multicomponent systems, it should be established when a chemical species is better described as a single (albeit large) molecule or as made of distinct molecular components (supermolecule).[7,10-12] From a photochemical and electrochemical viewpoint the distinction between a large molecule and a supramolecular species can be based on the degree of interaction between the electronic subsystems of the component units.[7,10] When the interaction energy between subunits is small compared to other relevant energy parameters, the system can be considered a supramolecular species. As shown in Scheme 1,[10] light excitation of a supramolecular species A~B (where ~ indicates any type of "bond" that keeps together the A and B subunits) leads to excited states that are substantially localized on A or B, or causes an electron transfer from A to B (or vice versa). When the excited states are substantially delocalized on both A

and B, the species is better considered as a large molecule. Similarly, oxidation and reduction of a supramolecular species can substantially be described as oxidation and reduction of specific components (Scheme 1), whereas oxidation and reduction of a large molecule leads to species where the hole or the electron are substantially delocalized on the entire system. (For other details on the electronic localization/delocalization problem, see section 4.2.)

In principle, the properties of the molecular components of a supramolecular species can be obtained from the study of the isolated components or of suitable model molecules. In several cases, however, the identification of real molecules that constitute suitable models for molecular components of a supramolecular species is not a trivial problem. Strictly speaking, in a covalent A–L–B species in which A and B are active components and L is a connector, A and B would be radicals or coordinatively unsaturated species that can never exist as such. In some cases, e.g. when the connector is bound to the components via carbon–carbon bonds, this is not a problem since molecular species such as AH and BH or AR and BR (R = alkyl group) will indeed show almost identical properties as A and B in the supramolecular species. In other cases, however, the connector may interact more deeply with the electronic subsystem of the active components. In such a case, compounds that include the connector, such as A–L and B–L, should be used to approach the properties of A and B in the supramolecular species.

4. Energy- and Electron-Transfer Processes

In a supramolecular species P–L–Q, where a photosensitizer P and a quencher Q are covalently linked by a component L, light excitation of P (eq 1) can be followed by energy (eq 2) or electron (eq 3) transfer processes. (In eq 3 and elsewhere we have schematized the case in which *P plays the role of electron donor; it is understood that it could also play the role of electron acceptor).

$$P\text{–}L\text{–}Q + h\nu \rightarrow {}^*P\text{–}L\text{–}Q \quad (1)$$

$${}^*P\text{–}L\text{–}Q \rightarrow P\text{–}L\text{–}{}^*Q \quad (2)$$

$${}^*P\text{–}L\text{–}Q \rightarrow P^+\text{–}L\text{–}Q^- \quad (3)$$

Light excitation can also cause electron transfer directly (optical electron transfer):

$$P\text{–}L\text{–}Q + h\nu \rightarrow P^+\text{–}L\text{–}Q^- \quad (4)$$

In the absence of interactions with other species, energy transfer will be followed by the radiative or radiationless decay of the acceptor excited state (eq 5),

$$P\text{–}L\text{–}{}^*Q \rightarrow P\text{–}L\text{–}Q + h\nu \text{ or heat} \quad (5)$$

while photoinduced (eq 3) and optical (eq 4) electron transfer will be followed by a thermal back-electron-transfer process:

$$P^+\text{–}L\text{–}Q^- \rightarrow P\text{–}L\text{–}Q \quad (6)$$

The relationships between optical, photoinduced, and thermal back-electron-transfer processes in supramolecular species are schematized in Figure 2.[7]

4.1. Electron Transfer

In an absolute rate formalism (Marcus model[60]), the rate constant for an electron-transfer process between

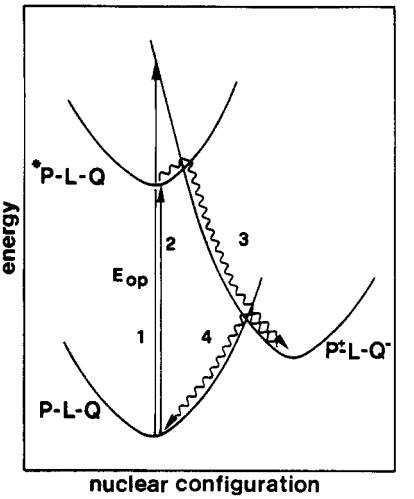

Figure 2. Relationship between optical (1), photoinduced (2 and 3), and thermal (4) electron-transfer processes in a supramolecular system. For the sake of simplicity, the vibrational levels are omitted.

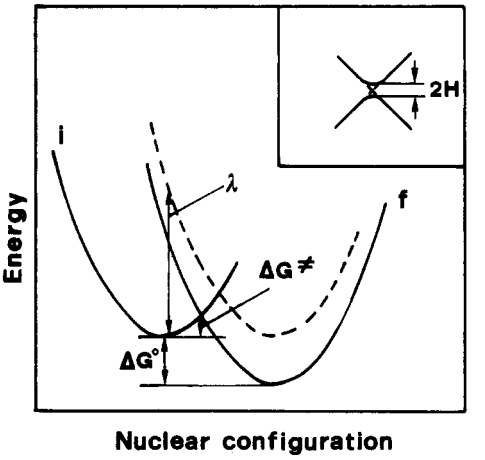

Figure 3. Profile of the potential energy curves of an electron-transfer reaction: i and f indicate the initial and final states of the system. The dashed curve indicates the final state for a self-exchange (isoergonic) process.

the components of a supramolecular system can be expressed as[61,62]

$$k = \nu_N \kappa \exp(-\Delta G^{\ddagger}/RT) \quad (7)$$

where ν_N is the effective nuclear frequency factor, κ is the electronic transmission coefficient, and $\Delta G^{\ddagger}$ is the free activation energy. This last term can be expressed by the Marcus quadratic relationship

$$\Delta G^{\ddagger} = \left(\frac{\lambda}{4}\right)\left(1 + \frac{\Delta G^{\circ}}{\lambda}\right)^2 \quad (8)$$

where ΔG° is the standard free energy change of the reaction and λ is the nuclear reorganizational energy (Figure 3). This equation predicts that for a homogeneous series of reactions (i.e., for reactions having the same λ and κ values) a log k vs ΔG° plot is a bell-shaped curve involving (i) a "normal" region for endoergonic and slightly exoergonic reactions in which log k increases with increasing driving force, (ii) an activationless maximum for $\lambda = -\Delta G^{\circ}$, and (iii) an "inverted" region, for strongly exoergonic reactions, in which log k *decreases* with increasing driving force.

The reorganizational energy λ can be expressed as the sum of two independent contributions correspond-

ing to the reorganization of the "inner" (bond lengths and angles within the two reaction partners) and "outer" (solvent reorientation around the reacting pair) nuclear modes:

$$\lambda = \lambda_i + \lambda_o \tag{9}$$

The outer reorganizational energy, which is the predominant term for electron-transfer processes in polar solvents, can be calculated by the expression[62]

$$\lambda_o = e^2\left(\frac{1}{\epsilon_{op}} - \frac{1}{\epsilon_s}\right)\left(\frac{1}{2r_P} + \frac{1}{2r_Q} - \frac{1}{r_{PQ}}\right) \tag{10}$$

where e is the electronic charge, ϵ_{op} and ϵ_s are the optical and static dielectric constants of the solvent, r_P and r_Q are the radii of the reactants, and r_{PQ} is the interreactant center-to-center distance. Equation 10 shows that λ_o is particularly large for reactions in polar solvents between reaction partners which are separated by a large distance. It should be pointed out that such an equation has been drawn according to a model which treats the interacting centers as spheres embedded in a dielectric continuum. (An alternative approach uses a low dielectric ellipsoidal cavity model, which better approximates the geometric properties of two-center species.[63]) Following the simplified approach of eq 10, the two centers are taken as electronically isolated so that a unit electronic charge, e, is transferred over the geometric center-to-center distance, r_{PQ}. However, careful evaluation of λ_o requires knowledge of (i) the actual amount of transferred charge over (ii) the actual distance of transfer. In principle, the two parameters could be evaluated according to a Mulliken-type approach for charge-transfer interactions.[64] In this case, one typically obtains the transition moment associated with electron transfer, $\mu = \alpha ed$, where α is a coefficient related to the initial state/final state electronic mixing. Recent studies on optical electron-transfer processes[65,66] and Stark effect measurements[67] on strongly-coupled mixed-valence systems indicate that either (i) a fraction of the electron charge (instead of unit charge) is transferred and/or (ii) the trapping sites are describable as electronic fragments closer to each other than suggested by the geometric description. An important consequence is that in such cases λ_o is remarkably smaller than evaluated on the basis of the simple use of eq 10 (section 12.4.1).

According to current theories,[18,62] the rate of an electron-transfer process in the nonadiabatic limit can be expressed by the following equation

$$k = \nu \exp(-\Delta G^{\ddagger}/RT) \tag{11}$$

where ν is an electronic frequency given by

$$\nu = \frac{2(H)^2}{h}\left(\frac{\pi^3}{\lambda RT}\right)^{1/2} \tag{12}$$

and H is the electronic interaction (Figure 3). The value of H depends on the overlap between the electronic wave functions of the donor and acceptor groups, that should decrease exponentially with donor–acceptor distance.

It should be noticed that the amount of electronic interaction required to promote photoinduced electron transfer (eq 3) is very small in a common chemical sense. In fact, it can be easily verified by substituting reasonable numbers for the parameters in eq 11 that, for an activationless reaction, H values of a few wavenumbers are sufficient to give rates in the subnanosecond time scale, while a few hundred wavenumbers may be sufficient to reach the limiting adiabatic regime ($\nu = \nu_N$).

As mentioned above, the connector is expected to play an important role in governing the electronic interaction between distant partners. In fact, depending on its length and electronic structure, the connector can induce a more or less important degree of delocalization between the active components, thus increasing H with respect to the corresponding intercomponent value at the same center-to-center distance. The role of the connector in enhancing the electronic coupling between the active components in a supramolecular system can be described in terms of "superexchange".[68–73] This through-bond mechanism can be viewed in terms of configuration interaction between the initial (P–L–Q) and final (P^+–L–Q^-) zero-order states of the electron-transfer process and high-energy charge-transfer states involving the bridging ligand, such as P^+–L^-–Q and P–L^+–Q^-.

It should also be noticed that the classical treatment neglects the role played by high-energy frequency vibrations as accepting modes. A simple quantum mechanical model treats the electron-transfer process as an activated radiationless transition beween different electronic states of the supermolecule, leading to a golden-rule expression[62]

$$k = (2\pi/\hbar)H^2\text{FCWD} \tag{13}$$

where the FCWD term is the Franck–Condon weighted density of states. In a simple approximation in which the solvent modes (average frequency, ν_o) are thermally excited and treated classically ($h\nu_o \ll k_BT$), and the internal vibrations (average frequency, ν_i) are frozen and treated quantum mechanically ($k_BT \ll h\nu_i$), the FCWD term is given by[74]

$$\text{FCWD} = \frac{1}{(4\pi\lambda_o RT)^{1/2}} e^{-S}\sum_m \frac{S^m}{m!}\exp\left[-\frac{(\Delta G^\circ + \lambda_o + mh\nu_i)^2}{4\lambda_o RT}\right] \tag{14}$$

$$S = \lambda_i/h\nu_i$$

In eq 14, λ_o and λ_i are the outer and inner reorganizational energies, and the summation extends over m, the number of quanta of the inner vibrational mode in the product state. It can be shown that, in the high-temperature limit, eqs 13 and 14 reduce to eq 15,

$$k = (2\pi/\hbar)H^2(4\pi\lambda RT)^{-1/2}\exp[-(\Delta G^\circ + \lambda)^2/4\lambda RT] \tag{15}$$

where $\lambda = \lambda_o + \lambda_i$.[74] By comparison with eqs 8, 11, and 12 it is seen that the high-temperature limit of the quantum mechanical expression corresponds to the *nonadiabatic* limit of the classical Marcus theory, in which the electronic coupling is small and the rate-determining step is electron rather than nuclear motion. In this limit the FCWD term in eq 13 corresponds to the exponential term of the classic rate constant (eq 11). Besides the inherent nonadiabaticity of the quantum mechanical mode, an important difference

between the quantum mechanical and the classical models is that eq 13 allows for *nuclear tunneling* between reactant and product levels at energies lower than that of the intersection point. This difference is especially relevant to the behavior predicted for highly exoergonic reactions, for which the parabolic behavior of the Marcus inverted region is substituted by a linear decrease of log k with increasing driving force (energy-gap law).[62,74]

4.2. Optical Electron Transfer

The Marcus model makes it clear that reactants and products of an electron-transfer process are intertwined by a ground/excited-state relationship. For example, for nuclear coordinates that correspond to the equilibrium geometry of the reactants, P^+–L–Q^- is an electronically excited state of P–L–Q (Figure 2). Therefore, optical transitions connecting the two states are possible, as indicated by arrow 1 in Figure 2.

The Hush theory[75] correlates the parameters that are involved in the corresponding thermal electron-transfer process by means of eqs 16–18

$$E_{op} = \lambda + \Delta G^\circ \tag{16}$$

$$\Delta\bar{\nu}_{1/2} = 48.06(E_{op} - \Delta G^\circ)^{1/2}\ (\mathrm{cm}^{-1}) \tag{17}$$

$$\epsilon_{max}\Delta\bar{\nu}_{1/2} = H^2\frac{r^2}{4.20\times 10^{-4}E_{op}} \tag{18}$$

where E_{op}, $\Delta\bar{\nu}_{1/2}$, and ϵ_{max} are the energy, halfwidth, and maximum intensity of the (Gaussian) electron-transfer band, and r the center-to-center distance (in Å). As shown by eqs 16–18, the energy depends on both reorganizational energy and thermodynamics, the halfwidth reflects the reorganizational energy, and the intensity of the transition is mainly related to the magnitude of the electronic coupling between the two redox centers.

In principle, therefore, important kinetic information on a thermal electron-transfer process could be obtained from the study of the corresponding optical transition. In practice, due to the dependence of the intensity on H, optical electron-transfer bands may only be observed in systems with relatively strong intercomponent electronic coupling. (For example for H values of 10, 100, and 1000 cm^{-1}, ϵ_{max} values of 0.2, 20, and 2000, respectively, are obtained from eq 18 using E_{op} = 15 000 cm^{-1}, $\Delta\bar{\nu}_{1/2}$ = 4000 cm^{-1}, and r = 7 Å). By recalling what is said in section 4.1, it is clear that weakly coupled systems may undergo relatively-fast electron-transfer processes without exhibiting appreciably-intense optical electron-transfer transitions.

Besides optical electron-transfer absorption, the possibility of optical electron-transfer emission should also be considered in the case of an electron-transfer process in the inverted region. Emissions of this type have been reported for covalently-bound organic donor–acceptor systems,[76] as well as for ion pairs.[77]

Optical electron-transfer transitions have been particularly investigated in mixed-valence dinuclear metal complexes such as 1, where L is a neutral, symmetrical bridging ligand.[78] In a valence-localized description, that is in terms of integral oxidation states of the metal centers, the overall charge corresponds to a Ru^{II}–Ru^{III} complex. In a fully delocalized description, on the other hand, a $Ru^{III/2}$–$Ru^{III/2}$ complex would result. The factors determining the localized or delocalized nature of the complex can be easily appreciated by following the approach originally developed by Hush.[75] Consider the two valence-localized "electronic isomers" Ru^{II}–Ru^{III} and Ru^{III}–Ru^{II}. A specific equilibrium geometry corresponds to each of these species, in terms of both *inner* and *outer* nuclear degrees of freedom. Figure 4a emphasizes the fact that at the equilibrium geometry of each electronic isomer the other isomer can be considered as an electronically excited state. The energy separation between these two states at the equilibrium geometry is the previously discussed reorganizational energy λ. At the crossing point both electronic isomers have the same energy and geometry. This is the nuclear configuration where there are no Franck–Condon restrictions to electron exchange between the two centers.

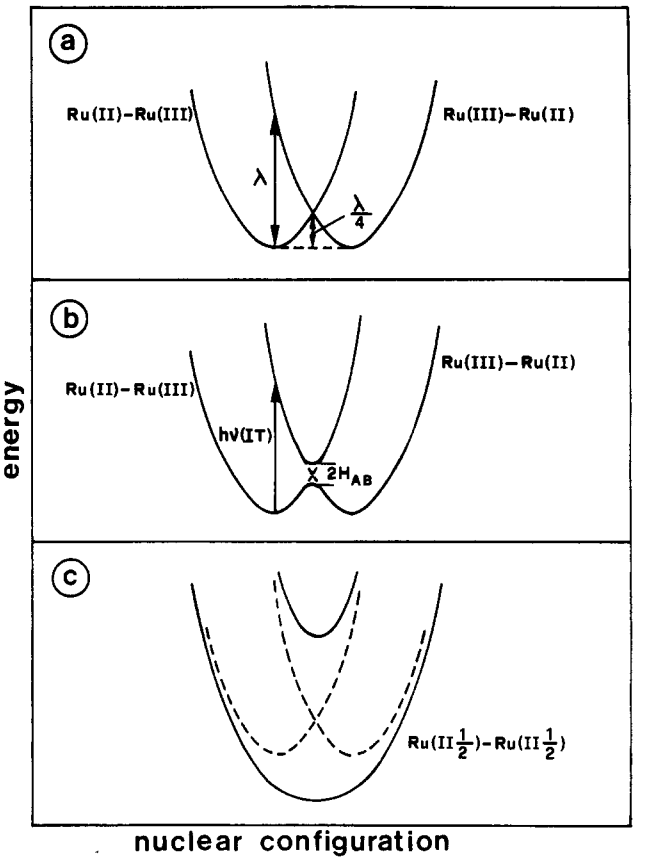

Figure 4. Potential energy curves for mixed-valence compounds with negligible (a), weak (b), and strong (c) electronic coupling. In b and c, the dashed curves represent zero-order states.

If for some reason (for example, very long center-to-center distance or insulating character of L) the electronic interaction between the Ru^{II} and Ru^{III} centers, H, is negligible, the curves in Figure 4a adequately represent the system at any geometry along the nuclear coordinate. For instance, the system 1 could be expected to exhibit properties which are a perfect superposition of the properties of isolated $Ru(NH_3)_5L^{3+}$ and $Ru(NH_3)_5L^{2+}$ components. Furthermore, even if the system acquires sufficient activation energy to reach the intersection region, the probability of electron exchange is negligible. In the field of mixed-valence chemistry, this is usually called class I behavior.[79] An

example approaching this type of behavior within the complexes of type 1 is obtained when L is the bridge 2.[78]

$$[Ru(NH_3)_5-L-Ru(NH_3)_5]^{5+}$$

1

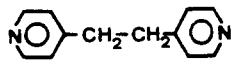

2

In most cases, however, some electronic interaction is likely to occur between the Ru^{II} and Ru^{III} centers, either as a consequence of direct orbital overlap or via some through-bridge mechanism. In such cases, the curves in Figure 4a are only zero-order representations. The electronic interaction has almost no effect on the zero-order curves in the vicinity of the equilibrium geometries, where the difference in energy between the electronic isomers is much larger than H, but causes mixing of the zero-order states (avoided crossing) in the vicinity of the crossing point (Figure 4b). Systems of this type can still be considered as valence-localized and will still exhibit the properties of the isolated $Ru(NH_3)_5L^{3+}$ and $Ru(NH_3)_5L^{2+}$ components. However, new properties promoted by the Ru^{II}–Ru^{III} interaction can also be observed, such as, for example, optical electron transfer with $h\nu = \lambda$. Such a transition clearly exchanges the valence of the two metal ions (i.e., it interconverts the two electronic isomers) and is therefore called *intervalence transfer* (IT) transition. The barrier to thermal electron transfer is only negligibly smaller than that calculated on the basis of the zero-order curves ($\lambda/4$). This type of behavior is usually called class II.[79] An example of class II behavior is obtained when L is the bridge 3.[78]

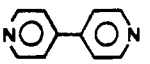

3

If strong electronic coupling is provided by the bridging ligand, the zero-order levels can be substantially perturbed even in the vicinity of their equilibrium geometries. In the limit of very large electronic coupling, when $H \simeq \lambda$, the true first-order curves will show a single minimum at an intermediate geometry (Figure 4c). In this case, the binuclear complex is better considered a fully delocalized $Ru^{III1/2}$–$Ru^{III1/2}$ species, with properties that are mostly unrelated to those of the hypothetical $Ru(NH_3)_5L^{3+}$ and $Ru(NH_3)_5L^{2+}$ components. This case is commonly indicated as class III.[79] An example of class III behavior within complexes of type 1 is obtained when L is the bridge 4.[78]

$$N\equiv C-C\equiv N$$

4

The above classification of mixed-valence compounds has been illustrated using symmetric redox sytems, that is systems made of identical subunits in which there is no net driving force for intramolecular electron transfer. The arguments concerning the degree of electron delocalization are, however, general and can be easily extended to systems which exhibit redox asymmetry. Clearly, mixed-valence class I and II compounds belong to our operational definition of "supermolecule" (section 3), while class III systems approach the "large molecule" limit.

4.3. Energy Transfer

Electronic energy-transfer processes can occur by two mechanisms:[7] the Förster-type mehanism,[80] based on Coulombic interactions, and the Dexter-type mechanism,[81] based on exchange interactions. The Förster-type mechanism is a long-range mechanism (its rate falls off as r^6, where r is the separation distance between donor and acceptor), which is efficient when the radiative transitions corresponding to the deactivation and the excitation of the two partners have high oscillator strength. The Dexter-type mechanism is a short-range mechanism (its rate falls off as e^r) that requires orbital overlap between donor and acceptor. When the donor and acceptor are linked together by chemical bonds, the exchange interaction can be enhanced by the above-mentioned (section 4.1) superexchange mechanism.

The rate of energy transfer according to the Förster mechanism can be calculated on the basis of spectroscopic quantities by

$$k_{en} = (5.87 \times 10^{-25})(\Phi_P/n^4\tau_P r^6) \int_0^\infty F_P(\bar{\nu})\epsilon_Q(\bar{\nu})\, d\bar{\nu}/\bar{\nu}^4 \quad (19)$$

where Φ_P and τ_p are the luminescence efficiency and lifetime of the donor excited state, respectively, n is the refractive index of the solvent, and the integral is related to the overlap between donor (P) emission and acceptor (Q) absorption. The rate constant for electron-exchange energy transfer may be expressed in a formalism[82–85] analogous to that used for electron-transfer processes.

5. Bis(terpyridine)–Metal Complexes as Photosensitizers

The free-energy change in an energy transfer process (eq 2) can be approximated as the difference in the zero–zero spectroscopic energies of the donor and acceptor excited states. For electron-transfer processes, the free-energy change is related to the redox potentials of the two couples. When a couple involves an excited state (eq 3), its redox potential can be approximated by the following equations

$$E°(*P/P^-) = E°(P/P^-) + E(*P) \quad (20)$$

$$E°(P^+/P*) = E°(P^+/P) - E(*P) \quad (21)$$

where $E°(P/P^-)$ and $E°(P^+/P)$ are the standard reduction potentials for the couples involving the ground-state component and $E(*P)$ is the one-electron potential corresponding to the zero–zero spectroscopic energy of the excited state.[86]

Figure 5 schematizes the processes taking place when an excited component *P is involved in energy or electron transfer.[86,87] It should be pointed out that in complexes of heavy metals only the lowest (formally spin-forbidden) excited state (*P in Figure 5) lives long enough to give rise to intercomponent energy- and electron-transfer processes. Such a state is usually

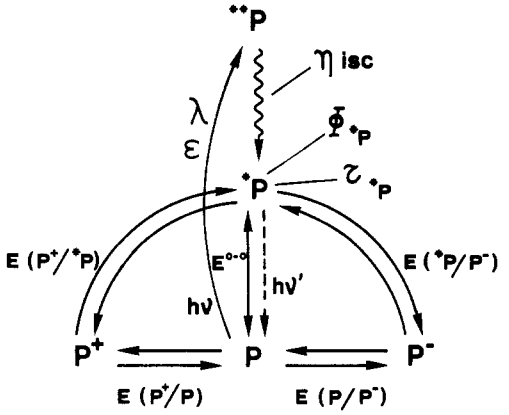

Figure 5. Schematic diagram showing the processes in which a photosensitizer (P) can be involved.

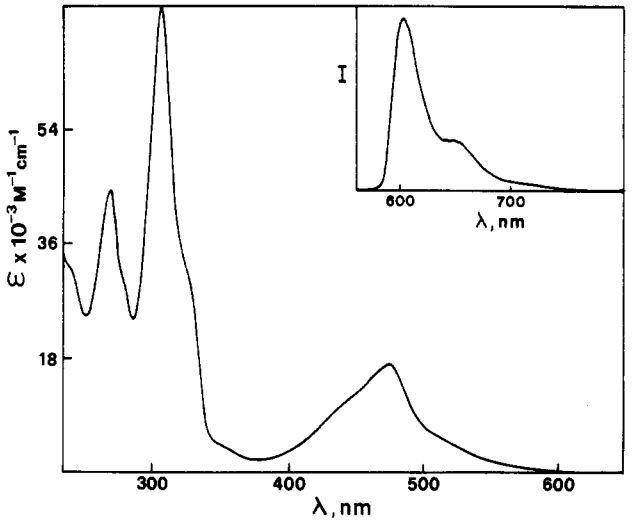

Figure 6. Absorption spectrum of $Ru(tpy)_2^{2+}$ in acetonitrile solution at room temperature. The inset shows the luminescence spectrum at 77 K.

populated via excitation to upper lying excited states (**P in Figure 5).

5.1. Ru(II) Complexes

The absorption spectrum of the prototype $Ru(tpy)_2^{2+}$ complex is shown in Figure 6. The very intense bands in the UV region can be assigned to ligand-centered $\pi \rightarrow \pi^*$ transitions. The relatively intense and broad absorption band in the visible region, which is responsible for the deep red color, is due to a spin-allowed d $\rightarrow \pi$ metal-to-ligand charge transfer (MLCT) transitions.[88]

In rigid matrix at 77 K $Ru(tpy)_2^{2+}$ exhibits a strong, long-lived luminescence characteristic of a triplet metal-to-ligand charge transfer (^{3}MLCT) level (Figure 6, inset). From the maximum of the luminescence band, the energy of the lowest excited state results to be 2.07 eV. On increasing temperature, the $Ru(tpy)_2^{2+}$ luminescence intensity and lifetime decrease. At room temperature, $Ru(tpy)_2^{2+}$ is practically not luminescent[88-93] and its excited-state lifetime, estimated to be 1.5 ns by flash photolysis.[89,90,93] was later found to be 250 ps from excited-state absorption.[94]

The anomalously weak emission of $Ru(tpy)_2^{2+}$ at room temperature compared with the strong emission of most ruthenium(II) polypyridine complexes was first attributed to the equilibration of the ^{3}MLCT state with high-spin d–d (metal centered, MC) states.[95] Another interpretation inferred that the terminal pyridines of tpy were relatively weakly bound in $Ru(tpy)_2^{2+}$ and subject to photodissociation in solution.[96] Presumably photodissociation could occur directly from the CT state. Reattachment to give the fully chelated form would complete a photochemical route to efficient nonradiative decay. Meyer and co-workers later suggested that the unfavorable bite angles associated with the tpy ligand result in a relatively weak ligand field in $Ru(tpy)_2^{2+}$ such that low-lying MC states are available to quench the luminescent ^{3}MLCT state.[97] Indication of the deviation from idealized octahedral geometry has in fact been found from X-ray structures.[98-100]

The quenching of ^{3}MLCT emission by neighboring ^{3}MC states is now a general and well-recognized phenomenon for ruthenium(II) polypyridine complexes.[86b] Some idea of the gap that separates ^{3}MC and ^{3}MLCT states for $Ru(tpy)_2^{2+}$ can be ascertained from the activation energy, $\Delta E = 1500$ cm^{-1}, obtained from temperature-dependent lifetime data.[92] This value is considerably smaller than that found for $Ru(bpy)_3^{2+}$, 4000 cm^{-1}.[86b]

Equations 22–24

$$^3\text{MLCT} \xrightarrow{k_a} {}^3\text{MC} \tag{22}$$

$$^3\text{MC} \xrightarrow{k_{-a}} {}^3\text{MLCT} \tag{23}$$

$$^3\text{MC} \xrightarrow{k_b} \text{GS} \tag{24}$$

describe the minimal decay scheme that allows for deactivation via a ^{3}MC state, where the k_b step represents decay to the ground state (GS). Since the ^{3}MC state is a short-lived state that is populated via a thermally activated process, it can be regarded as a steady-state species. In such a case the rate constant for decay through this channel can be written as

$$k = k_a \frac{k_b}{k_{-a} + k_b} \tag{25}$$

Limiting cases of eq 25 have been discussed in detail.[86b] Case I behavior is obtained when $k_b \gg k_{-a}$. In this limit, the rate constant for the relaxation process in question is effectively k_a. The ΔE process has a frequency factor of the order of 10^{13} s^{-1}, which is consistent with a simple barrier crossing (case I) process. Accordingly, ΔE is taken to be the barrier associated with crossing from the ^{3}MLCT to the short-lived ^{3}MC state. In the light of these results, it is surprising the fact that theoretical calculations would indicate that the ^{3}MC level lies far above the ^{3}MLCT state.[101]

Photoanation of $Ru(tpy)_2^{2+}$ is almost negligible in CH_2Cl_2 solution with added SCN^-, but it occurs with moderate quantum yields for $Ru(6,6''\text{-dptpy})_2^{2+}$ with formation of an η^2-diphenylterpyridine (η^2-dptpy) complex.[91]

In the last few years a great number of tpy derivatives have been used to prepare Ru(II) complexes[88,91,92,94,99,101-114] (Table 1). $Ru(6,6''\text{-dptpy})_2^{2+}$ is unique in that it does not show any luminescence even at 77 K. A plausible explanation is the presence of interligand steric repulsions which further weaken the ligand field.[91] As a consequence, the ^{3}MC state may

Table 1. Absorption, Luminescence, and Electrochemical Data

complexes	absorption[a] λ, nm (ε, M^{-1} cm^{-1})	emission (298 K)[a] λ, nm	φ	τ, ns	emission (77 K)[a] λ, nm	φ	τ, μs	electrochemistry:[b] $E_{1/2}$, V 2+/1+	1+/0	ref(s)
$Ru(tpy)_2^{2+}$	476 (17 700)	–		0.250	598	0.48	11	+1.30	−1.24	88,94,102
$Ru(Cl\text{-}tpy)_2^{2+}$	480 (16 000)[c]	630[c]	$<10^{-5}$ [c]	1.0[c]	615[c]		8.6[c]	+1.0[d]	−1.53[d]	99,103
$Ru(Me_2N\text{-}tpy)_2^{2+}$	490 (15 400)[c]				656[c]		5.4[c]	+0.42[d]	−1.90[d]	99,103
$Ru(HO\text{-}tpy)_2^{2+}$	485 (12 700)[c]				620[c]		6.6[c]	+0.73[d]	(−1.81)[d]	99,103
$Ru(MeSO_2\text{-}tpy)_2^{2+}$	485[c]	650[c]	4×10^{-4} [c]	25[c]	632[c]		10.5[c]	+1.1[d]		103
$Ru(EtO\text{-}tpy)_2^{2+}$	485 (17 500)[c]				618[c]		6.4[c]	+0.74[d]	−1.76[d]	104
$Ru(ph\text{-}tpy)_2^{2+}$	488 (30 000)[c]	670[c]	2×10^{-5} [c]		632[c]		10.5[c]	+0.90[d]	−1.66[d]	104
$Ru(Cl\text{-}phtpy)_2^{2+}$	490 (24 600)	645	4×10^{-5}	11						101
$Ru(HO\text{-}phtpy)_2^{2+}$	496 (26 100)									101
$Ru(MeO\text{-}phtpy)_2^{2+}$	495 (24 400)	650	3×10^{-5}	4.8	632	0.4	13			101
$Ru(tphtpy)_2^{2+}$	501 (38 400)	650	7.4×10^{-4}	3.8	633	0.57	7.8	+1.22	−1.19	88,102
$Ru(4,4'\text{-}dptpy)_2^{2+}$	495 (28 300)		1.5×10^{-4}	4.0						92
$Ru(6,6''\text{-}dptpy)_2^{2+}$	477 (6 850)[e]									91
$Ru(ttpy)_2^{2+}$	490 (28 000)[c]	640[c]	3.2×10^{-5} [c]	0.95[c]	628[c]		9.1[c]	+1.25	−1.24	105–107
$Ru(tppz)_2^{2+}$	478[c]	648			628			+1.51	−0.88	108,109
$Ru(tpy)(tppz)^{2+}$	470 (20 100)[c]	670		91[c]	600			+1.50	−0.95	108.109
$Ru(ttpy)(phbp)^{+}$	523 (9 960)[c]	808[c]	5×10^{-6} [c]	60[c]	792[c]	5×10^{-4} [c]	0.9[c]	+0.54		113
$Ru(ttpy)(dpb)^{+}$	550 (8 250)[c]	784[c]	1.8×10^{-5} [c]	1.5[c]	752[c]		0.48[c]	+0.49	−1.61	114
$Os(tpy)_2^{2+}$	657 (3 650), 477 (13 750)	718	0.014	269[c]	689	0.124	3.9	+0.97	−1.23	102,110,111
$Os(ttpy)_2^{2+}$	667 (6 600), 490 (26 000)[c]	734[c]	0.021[c]	220[c]	740[f]	0.049[f]	0.54[f]	+0.93	−1.23	102
$Os(tppz)_2^{2+}$	470 (20 100)[c]	731			740			+1.23	−0.83	108
$Os(tpy)(tppz)^{2+}$	470 (10 800)[c]	770			643			+1.08	−0.97	108
$Os(tphtpy)_2^{2+}$	692 (9 200), 502 (33 050)	751	0.028	266				+0.90	−1.15	102
$Os(ttpy)(dpb)^{+}$	765 (2 000), 537 (13 000)[c]	824[c]	0.9×10^{-6} [c]	<0.030[c]	832[c]			+0.34	−1.60	114

[a] In alcohol solution, unless otherwise specified. [b] In acetonitrile solutions, 298 K; $E_{1/2}$ values in volts, vs SSCE, unless otherwise specified. [c] Nitrile solvents. [d] Electrochemical potentials vs Fc/Fc^+ in acetonitrile solution. [e] In CH_2Cl_2. [f] In nitrile solvent at 155 K.

fall *below* the ^{3}MLCT state, so that emission is quenched at all temperatures. The same steric repulsions could explain the previously mentioned photoanation reaction.[91]

As one can see from Table 1, ligand substituents cause considerable variations in the absorption and luminescence properties. It is clear that phenyl substituents in the 4, 4′, and 4″ positions increase the molar absorption coefficient, as expected on simple theoretical grounds.[115] The substituent effect on the energy of the absorption and emission bands results from a combined perturbation of the LUMO (ligand π*) and HOMO (metal t_{2g}, in octahedral symmetry) orbitals.[104] The effect on the luminescence quantum yield and lifetime is likely related to the above-mentioned perturbations as well as to the substituent effect on the ligand field strength (and, as a consequence, on the ^{3}MLCT-^{3}MC energy gap, *vide supra*).[104] In general, (i) both the electron-withdrawing and -donating substituents stabilize the MLCT excited state, with a consequent red shift on the absorption and emission maxima, and (ii) the electron-withdrawing substituents increase the excited state lifetime and the luminescence intensity at room temperature.

The $Ru(tpy)_2^{2+}$-type complexes are electrochemically active. They exhibit a reversible $Ru^{II,III}$ oxidation process and a variable number of reversible or quasi-reversible reductive ligand-centered processes. Some of the electrochemical data are presented in Table 1. The presence of strongly electron-releasing substituents allows a stabilization of the Ru^{III} state and a shift of the oxidative process to less positive potentials. In the same way, electron-releasing substituents shift the reductive processes to more negative potentials. Correlations between electrochemical and excited-state properties have been found.[104]

5.2. Os(II) Complexes

In going from $Ru(tpy)_2^{2+}$ to $Os(tpy)_2^{2+}$, some important differences can be noticed as far as the excited state and redox properties are concerned.[102,110,111,116]

As one can see from the electrochemical data gathered in Table 1, the Os(II) complexes are oxidized at less positive potentials than the Ru(II) complexes, whereas the first reduction potential is almost the same in the two series of compounds.

Although Os(II) is easier to oxidize than Ru(II), the absorption maximum of the spin-allowed MLCT band in the visible region for $Os(tpy)_2^{2+}$ lies at the same wavelength as that of $Ru(tpy)_2^{2+}$. This could be due to a more covalent character of the metal–ligand interaction in the Os complex. For $Os(tpy)_2^{2+}$, the spin-forbidden MLCT band (λ_{max} = 657 nm) is quite intense, as expected because of the large spin–orbit coupling caused by the heavy Os atom. At 77 K, the luminescence band of $Os(tpy)_2^{2+}$ is considerably shifted to the red compared to that of $Ru(tpy)_2^{2+}$.[111] Contrary to what happens for $Ru(tpy)_2^{2+}$, $Os(tpy)_2^{2+}$ exhibits a relatively intense and long-lived luminescence even in fluid solution at room temperature (Table 1). This indicates that in the Os complex the short-lived ^{3}MC levels cannot be populated at room temperature. In $Os(tpy)_2^{2+}$, in fact, the ^{3}MLCT/^{3}MC energy gap is much higher than in the analogous Ru complex because of (i) the lower energy of the ^{3}MLCT level, due to the fact that Os(II) is easier to oxidize than Ru(II), and (ii) the higher energy of the ^{3}MC level, due to the stronger ligand field of Os(II) compared with Ru(II).[111]

5.3. Complexes of Other Metals

A few other $M(tpy)_2^{n+}$ complexes have been investigated from the point of view of their excited state behavior.

In the case of $Cr(tpy)_2^{3+}$, the lowest excited state is the ^2E MC level. The luminescence maximum lies at 775 nm, and the excited state lifetime is 50 ns.[117]

For $Fe(tpy)_2^{2+}$, no emission can be observed and an excited-state lifetime of 2.5 ns has been obtained from transient absorption spectroscopy in aqueous solution at room temperature.[93] It is believed that such an excited state has MC orbital nature, as expected because of the weak ligand field of Fe(II).

In the case of $Ir(tpy)_2^{3+}$, the MC levels lie at high energies because of the strong ligand field of Ir(III), and the MLCT levels are also expected to lie at high energies because Ir(III) is rather difficult to oxidize. As a consequence, the lowest excited state is a triplet ligand-centered (LC) level. $Ir(tpy)_2^{3+}$, in fact, exhibits a LC phosphorescence (λ_{max} = 455 nm),[118] slightly red-shifted compared to the LC phosphorescence displayed by $Zn(tpy)_2^{2+}$ (λ_{max} = 434 nm).[119] At room temperature, the lifetime of the ^3LC level of $Ir(tpy)_2^{3+}$ is 70 ns.[118]

6. Design of Multicomponent Systems

6.1. Geometry of the Photosensitizer

As mentioned in section 2, in multicomponent systems photoinduced charge separation and/or energy migration can only be achieved when the various molecular building blocks are assembled according to well-designed geometric patterns. At the present state of chemical research, the best route to assemble molecular building blocks according to a desired pattern is the use of a covalent bond. We will see, in fact, that preparation of the $M(tpy)_2$ core has two distinct functions: (i) synthesis of the photosensitizer itself, and (ii) gathering and orienting electroactive components attached to the two different tpy ligands.

The building blocks to be assembled must exhibit suitable photochemical, photophysical, and electrochemical properties. Key components are the photosensitizers, i.e. species capable of absorbing ligand and transferring energy, electron, or hole to another component.

On the basis of photochemical, photophysical, and electrochemical properties, Ru(II) and Os(II) complexes of 2,2′-bipyridine and related bidentate ligands (bpy-type ligands) are probably the best photosensitizers among metal complexes.[86,87,120] Especially in the case of Ru(II), several hundreds of bpy-type complexes have been prepared and characterized, thereby making available a wide choice of photosensitizer components for the design of PMDs based on photoinduced chargeseparation or energy migration. Although very interesting rod-like systems based on $Ru(bpy)_3^{2+}$ and $Os(bpy)_3^{2+}$ have recently been synthesized,[121,122] in terms of geometry the use of bidentate bpy-type ligands is much less convenient than the use of terdentate tpy-type ligands. This is apparent on looking at Figure 7, where the structures of $M(bpy)_3^{n+}$ and $M(tpy)_2^{n+}$ complexes and of their derivatives are illustrated.[123,124] 2,2′-Bipyridine gives rise to stereoisomerism at six-coordinated centers due to their bidentate nature. A $M(bpy)_3^{n+}$ complex exists in two enantiomeric forms. If the bpy ligand bears a single substituent, two geometrical forms with *facial* and *meridional* arrangements are found; each of this isomer can exist as one of two enantiomers. A further drawback is that with the basic $M(bpy)_3^{n+}$ arrangement the building up of supramolecular structures occurs with no control of isomer formation, leading to a mixture of triad systems where the two components linked to the photosensitizer can also occupy *cis* position.[125] In contrast to the behavior with bpy, a six-coordinate metal forms an achiral $M(tpy)_2^{n+}$ complex upon reaction with tpy. The introduction of a single substituent in the 4′ position of each tpy ligands presents no additional problems; there is a single form of the resulting complex. Furthermore the geometry of $M(tpy)_2^{n+}$ complexes offers the possibility to design triads in which the two additional components lie on opposite directions with respect to the photosensitizer (trans-type configuration, Figure 7).[123,126] This is due to the fact that the 4′ anchoring point of tpy belongs to the symmetry elements of the ligand and of the $M(tpy)_2^{n+}$ complex (two symmetry planes and three C_2 axes). Furthermore, the interposition of aromatic rings between the A or D components and tpy affords a very convenient way to increase the A–D separation distance.[127]

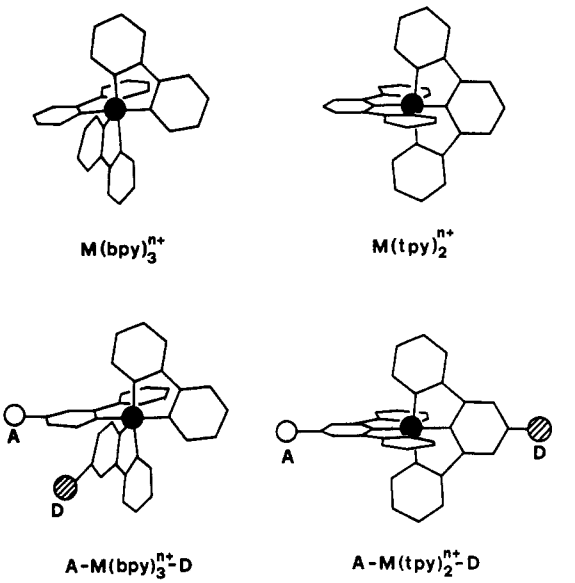

Figure 7. Schematic representations of $M(bpy)_3^{n+}$ and $M(tpy)_2^{n+}$ complexes and of their disubstituted derivatives.

Because of its geometry, tpy is also a good candidate to play the role of ligand in the binding sites of macrocyclic rings. In fact, a three-dimensional template synthesis of two interlocked tpy-containing macrocycles around a Ru(II) ion has been devised to prepare the first catenate containing an octahedral binding site.[128]

6.2. Electron Donors and Acceptors

In order to obtain photoinduced charge separation, the photosensitizer must be able to transfer an electron or hole to another component, as it happens in the reaction centers of the natural photosynthetic assemblies (section 2). Two-component systems (dyads) can be obtained by connecting the photosensitizer (P) either to an electron acceptor (A) or to an electron donor (D) having suitable redox properties (Figure 8). In such two-component systems the back-electron-transfer reaction (from A^- to P^+ in P–A and from P^- to D^+ in D–P, Figure 8) is usually too fast to allow any practical use of the charge-separation process. Systems containing three or more components are expected to be more

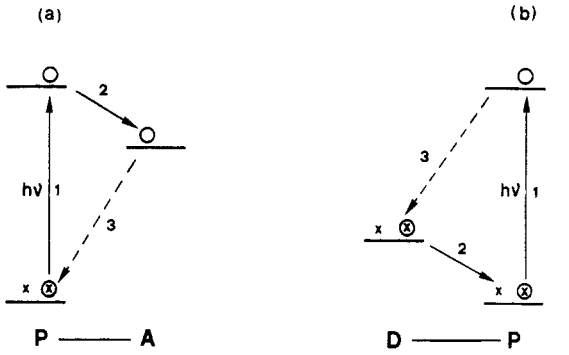

Figure 8. Schematic representation of the photoinduced charge-separation process in dyads. P is a photosensitizer, and A and D are an electron acceptor and donor, respectively. (a): 1, excitation; 2, transfer of the excited electron to the acceptor; 3, charge-recombination reaction. (b): 1, excitation; 2, transfer of an electron from the donor to the excited photosensitizer; 3, charge-recombination reaction.

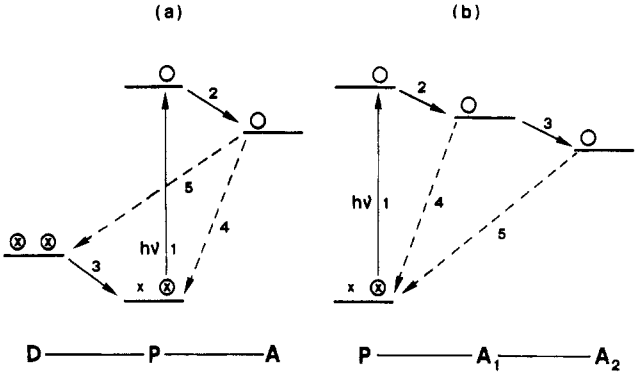

Figure 9. Schematic representation of the photoinduced charge-separation process in triads. P is a photosensitizer, D is an electron donor, and A, A_1, and A_2 are electron acceptors. (a): 1, excitation; 2, transfer of the excited electron to the acceptor; 3, transfer of an electron from the donor to the oxidized photosensitizer; 4, charge recombination whose occurrence prevents full charge separation; 5 charge-recombination reaction after full charge separation. (b): 1, excitation; 2, transfer of the excited electron to the primary A_1 acceptor; 3, transfer of the electron to the secondary acceptor A_2; 4, charge recombination whose occurrence prevents full charge separation; 5 charge-recombination reaction after full charge separation.

efficient because fast secondary electron-transfer step(s) can compete with the back-electron-transfer reaction(s), resulting in a charge separation over larger distances. As shown in Figure 9, two structures are possible for a triad: D–P–A and P–A_1–A_2 (or D_2–D_1–P). The above-described geometrical structure of the tpy-type ligands are particularly suitable for the D–P–A linear arrangement.

The donor and acceptor components should not absorb light of the wavelength used to excite the photosensitizer. They should exhibit appropriate redox potentials, a reversible redox behavior, and the oxidation of the donor and the reduction of the acceptor should be accompanied by intense absorption changes in appropriate spectral regions in order to detect the occurrence of electron transfer by flash spectroscopy. Since most of the molecules absorb in the UV region, the growth or disappearance of intense and narrow bands in the visible are quite useful. Time-resolved microwave conductivity measurements can also be used to detect the formation of a charge-separated state.[129]

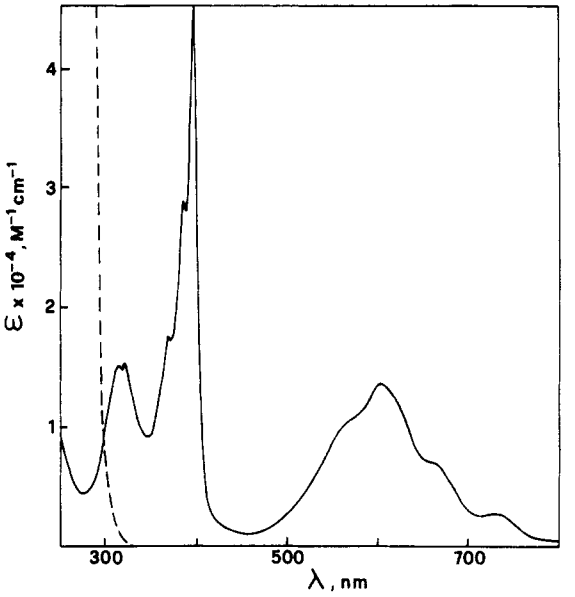

Figure 10. Absorption spectrum of MV^{2+} (dashed line) and MV^{+} (full line) in acetonitrile solution.

A limited number of electron donors and acceptors have been used so far. A systematic research aimed at the discovery or design of electron donors and acceptors capable of satisfying the above requirements would certainly give a strong contribution to the developments of PMDs. Presently, the most widely used electron acceptors are those of the viologen and quinone families. The spectral changes accompanying the reduction of MV^{2+} to MV^{+} are shown in Figure 10. The most common electron donors are amines. For instance, in systems based on coordination compounds, phenothiazine has been frequently used.[125] Ferrocene and its derivatives have also been extensively used as potential electron donors in view of their accessible oxidation potential and reversible redox behavior; these compounds, however, have low-energy excited states and therefore they can cause the quenching of the excited photosensitizer by energy transfer.[82,130–132]

6.3. Energy Acceptors

The components to be used as acceptors in energy transfer processes must also meet several requirements. They should possess excited levels at suitably low energies and should not undergo excited-state reactions. The most straightforward proof that energy transfer has occurred is the sensitized emission of the acceptor. Therefore, luminescent coordination compounds are commonly used as energy acceptors. Several supramolecular systems based on Re(I), Ru(II), Os(II), and Cr(III) complexes have been investigated.[133] Re(I) and Ru(II), which exhibit high-energy luminescent levels, usually play the role of photosensitizers, and Os(II) and Cr(III) complexes, whose luminescent levels lie at much lower energy, usually play the role of energy acceptors. Of course complexes of the same metal and different ligands can also be coupled for energy-transfer purposes.

6.4. Spacers

As mentioned in section 4, the spacers play a 2-fold role: (i) control of the supramolecular structure (in

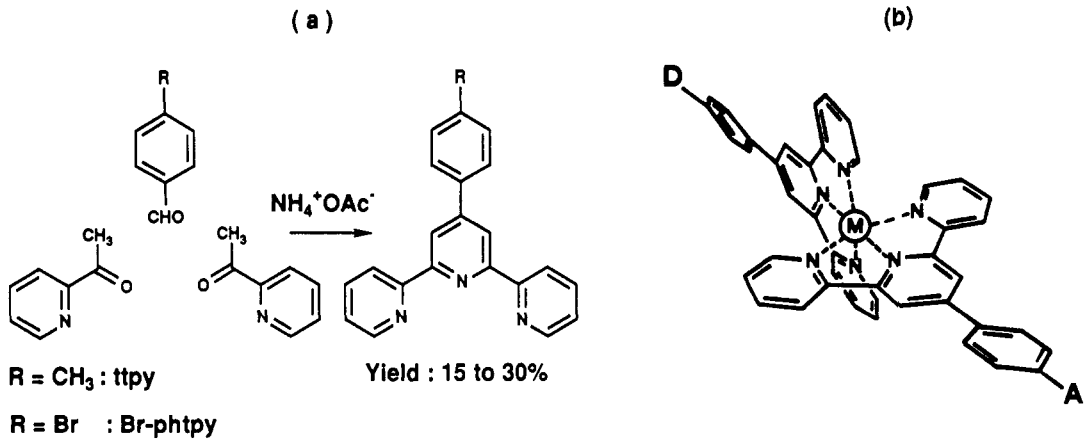

Figure 11. (a) Synthetic route to various substituted terpyridines; R can be CH_3, Br, OCH_3, etc. By appropriate chemical modifications, electron acceptor (A) and donor (D) groups can be introduced in the right positions of the ligands. (b) The triad compounds designed are rigid and ensure a minimum A–D distance (edge-to-edge) of 21 Å.

particular, of the intercomponent distances and angles); (ii) control of the electronic communication between components in case of through-bond energy or electron transfer. Obviously rigid spacers, such as those based on aromatic rings,[105,134] bicyclo aliphatic species,[121,122] and bridges containing ethynyl groups[135] should be preferred to flexible spacers (e.g., aliphatic chains) for structural reasons. From the electronic viewpoint, aromatic spacers allow a better communication than aliphatic ones, but a complete picture of the electronic effects of spacers has not yet been obtained.

7. Synthesis of the Ligands

7.1. Synthesis of Mono-tpy Ligands Bearing Electroactive Components

In order to synthesize tpy derivatives bearing various functional groups at the 4′ position, it is essential to have an efficient and flexible preparative method at disposal. Among the few synthetic routes available for making terpyridines,[136–139] the procedure developed long ago by Case et al.[136] and more recently improved by Swiss researchers[139] was selected. This approach allows gram-scale preparation of various 4′-aryl tpy's as indicated in Figure 11a. In this way the electroactive groups will be connected to the bis-tpy complexes by phenyl spacers, imposing a minimum edge-to-edge distance between D and A of 21 Å (Figure 11b).

Discussing in detail the organic synthesis of the ligands made[107,127,140] is beyond the scope of this review. It can just be noted that using the condensation reaction of Figure 11a, two general strategies have been adopted. One can prepare the tolyl derivative ttpy, convert the CH_3 group into a CH_2Br function, and use the latter for anchoring the desired electrophore. The other possibility is obviously to include the electroactive function into the aromatic aldehyde prior to the tpy formation reaction. Both routes have been explored and used, their choice being dictated by the chemical stability of the donor or the acceptor, since the second approach implies that the electrophore will have to resist the relatively harsh experimental conditions of the cyclization reaction.

The various ligands made are represented in Figure 12. They contain either D or A as pendant group.

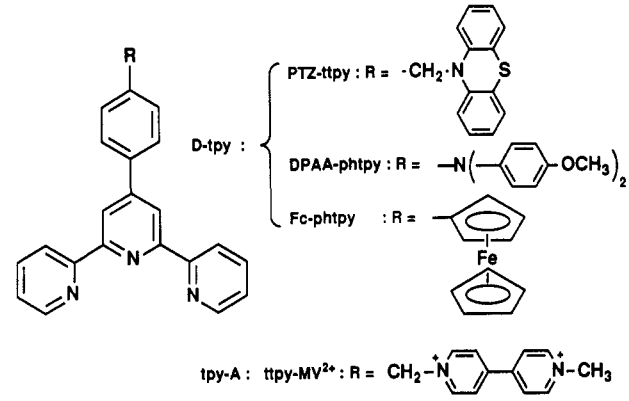

Figure 12. Various tpy derivatives used, with an electrophore rigidly attached to the chelate via a 1,4 phenylene spacer. PTZ = phenothiazine; DPAA = di-*p*-anisylamine; Fc = ferrocene; MV^{2+} = methylviologen.

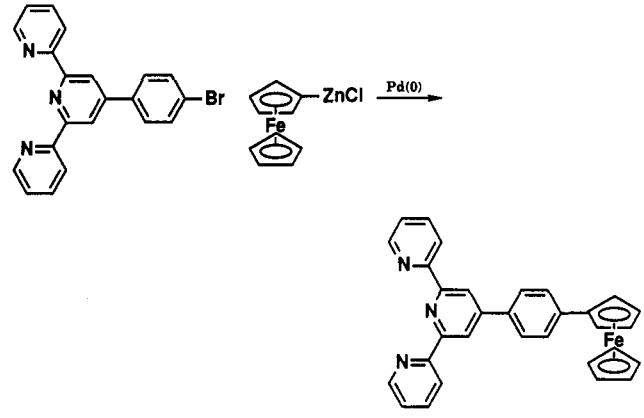

Figure 13. Preparation of the 4′-(*p*-ferrocenylphenyl)-2,2′:6′,2″-terpyridine. Pd(0) indicates a catalitic amount of palladium(0) complex.

The ligand Fc-phtpy was prepared in a different way.[140] As shown in Figure 13, Br-phtpy (4′-(*p*-bromophenyl)-tpy) was reacted with ferrocenylzinc chloride in the presence of a Pd(0) complex used as coupling catalyst to afford Fc-phtpy in 80% yield.

7.2. Synthesis of Bridging Bis-tpy Ligands

By connecting two terpyridine units via a rigid spacer attached to their 4′ positions, bridging ligands displaying axial symmetry can be obtained. The compounds

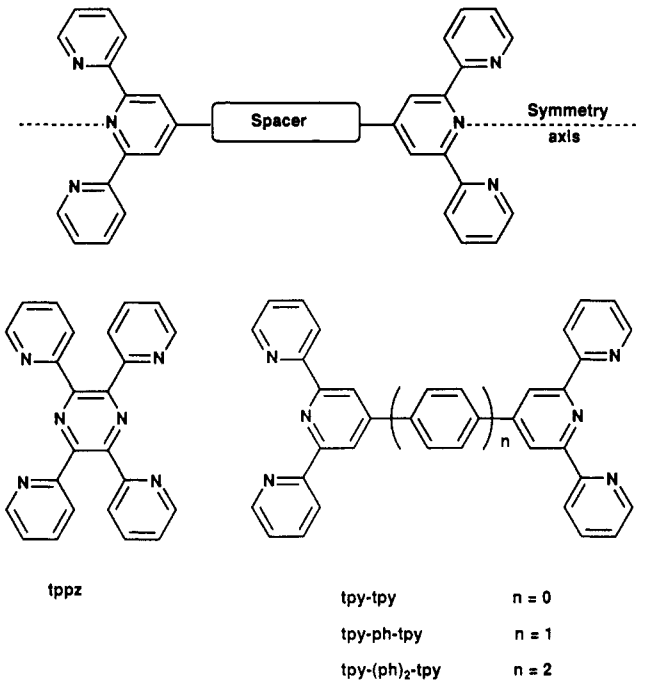

Figure 14. Ligands used in the preparation of the dinuclear complexes.

synthesized and used further to make dinuclear complexes are represented in Figure 14. The ligand tppz was prepared according to a procedure described long ago by Goodwin and Lions,[141] by condensing two molecules of pyridoin with ammonium acetate. The bis-tpy ligand tpy-tpy was synthesized by reductive coupling of 4′-chloro-2,2′:6′,2″-terpyridine, following the methodology recently reported by Constable and Ward.[142] The phenyl-bridged bis-tpy ligand tpy-ph-tpy was obtained according to the method developed by Kröhnke et al.[137] and also applied to the synthesis of a large variety of polypyridinic compounds. The same reaction has also been used more recently by others.[143] The principle is very general and can allow preparation of virtually any compound containing several pyridine nuclei attached to aromatic rings. The reaction sequence leading to tpy-ph-tpy is given in Figure 15. The biphenyl-containing ligand tpy-$(ph)_2$-tpy was obtained by homocoupling of 4′-(*p*-bromophenyl)-2,2′:6′,2″-terpyridine in the presence of nickel(0) triphenylphosphine complex and Zn dust in DMF. The high yield (~60%,) allows preparation of this bridging ligand at the gram scale.

It should be noted that the bromo-tpy used as starting material is readily available from 2-acetylpyridine and 4-bromobenzaldehyde[139] (Figure 11). Potentially this functionalized terpyridine is the ideal precursor to any bridging multi-tpy ligand. It should lead to bis-tpy systems with various aromatic or saturated spacers as well as to bridging multichelates by connecting several such tpy's.

8. Synthesis of Dyads and Triads Based on $Ru(tpy)_2^{2+}$-type Photosensitizers

Several dyads and triads based on $Ru(tpy)_2^{2+}$-type complexes as photosensitizers have been synthesized (Table 2). The ligands used are shown in Figure 12.

Table 2. Preparation of Dyads and Triads Based on $Ru(tpy)_2^{2+}$-type Complexes

complex	method	yield	ref(s)
(Fc-phtpy)Ru(ttpy)$^{2+}$	A	15%	140
(PTZ-ttpy)Ru(ttpy)$^{2+}$	A	5%	107
(DPAA-phtpy)Ru(ttpy)$^{2+}$	A	37%	107
(ttpy)Ru(ttpy-MV^{2+})$^{4+}$	B	8%	107, 127
(PTZ-ttpy)Ru(ttpy-MV^{2+})$^{4+}$	B	5%	107, 127
(DPAA-phtpy)Ru(ttpy-MV^{2+})$^{4+}$	B	8%	107
(Fc-phtpy)Ru(ttpy-MV^{2+})$^{4+}$	B	18%	140b

The dyads and triads have been prepared either in a *sequential manner* (A) or by a *statistical method* (B):

(A) $$RuCl_3 + ttpy \rightarrow Ru(ttpy)Cl_3$$

$$Ru(ttpy)Cl_3 + D\text{-}tpy \xrightarrow{(i)} (ttpy)Ru(tpy\text{-}D)^{2+}$$

(i): reflux in ethanol–water–triethylamine for 1 h

(B) $$\text{"ruthenium blue"} + L_1 + L_2 \xrightarrow{(ii)} Ru(L_1)_2^{2+} + Ru(L_1)(L_2)^{2+} + Ru(L_2)_2^{2+}$$

$(L_1)(L_2)$: (ttpy,ttpy-MV^{2+})
(PTZ-ttpy,ttpy-MV^{2+})
(DPAA-phtpy,ttpy-MV^{2+})

(ii): reflux in ethanol for 18 h

Method A can be used for ligands bonded to an electron donor (D-tpy). However, it is not appropriate for the synthesis of complexes containing the ttpy-MV^{2+} ligand. The triads and the electron-acceptor dyad (ttpy)Ru(ttpy-MV^{2+})$^{4+}$ must thus be prepared following the statistical procedure (B).

9. Synthesis of Dyads and Triads Based on $Os(tpy)_2^{2+}$-type Photosensitizers

Although the coordination sphere of ruthenium is considered to be relatively inert vis-à-vis substitution reactions, it is still very labile as compared to osmium. In fact, the substitution of ligands within the coordination sphere of osmium is notoriously difficult and requires either extremely brutal conditions or multistep procedures involving different metal oxidation states. Using the ligands of Figure 12, various osmium(II) complexes can be prepared.[112,127,140-144] Due to the chemical fragility of some of the ligands, the classical very drastic conditions consisting of heating osmium salts and ligands at very high temperature (typically, refluxing ethylene glycol) for long periods cannot be systematically applied. More elaborate, specific methods have thus been developed. Two general routes used are indicated in Figure 16.

The synthesized dyads and triads based on $Os(tpy)_2^{2+}$-type complexes are listed in Table 3. Importantly, since photophysical measurements are very sensitive to impurities, special care must be taken in order to isolate very pure samples of the various ruthenium(II) and osmium(II) complexes. For this purpose, a special chromatographic technique was developed and applied

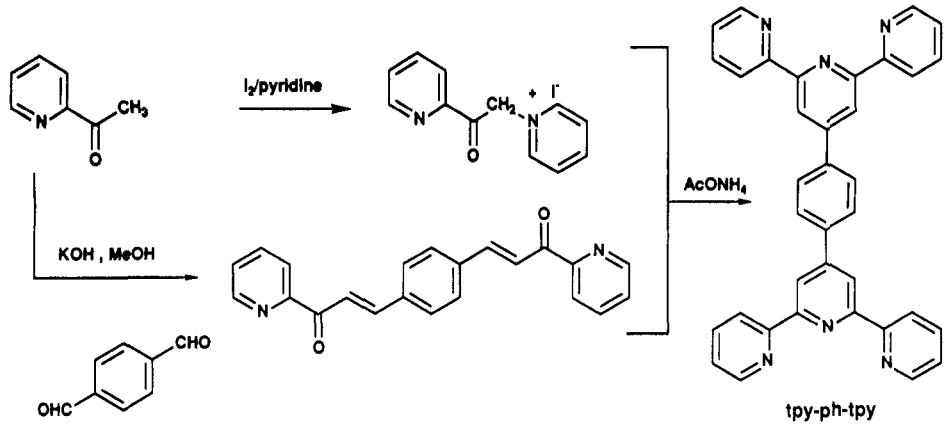

Figure 15. Preparation of tpy-ph-typ according to ref 137.

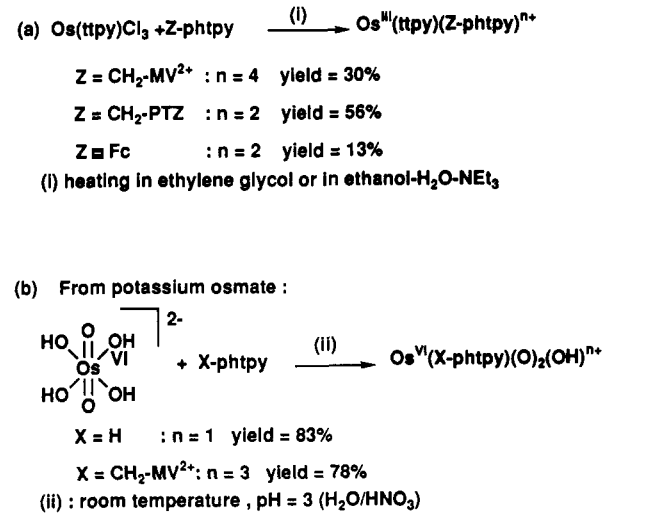

Figure 16. The two general routes to substituted bis(terpyridine)osmium(II) complexes.

Table 3. Preparation of Dyads and Triads Based on $Os(tpy)_2^{2+}$-type Complexes

complex	method (see Figure 18)	ref(s)
(ttpy)Os(ttpy-MV^{2+})$^{4+}$	A or B	127, 144
(PTZ-ttpy)Os(ttpy)$^{2+}$	A	127, 144
(Fc-phtpy)Os(ttpy)$^{2+}$	A	140
(DPAA-phtpy)Os(ttpy)$^{2+}$	B	144
(PTZ-ttpy)Os(ttpy-MV^{2+})$^{4+}$	B	112
(DPAA-phtpy)Os(ttpy-MV^{2+})$^{4+}$	B	112
(Fc-phtpy)Os(ttpy-MV^{2+})$^{4+}$	B	140b

to all the compounds prepared. Column chromatography was performed on silica gel, with a mixture of solvents (usually CH_3CN and H_2O) containing a salt (KNO_3, for instance) as eluent.

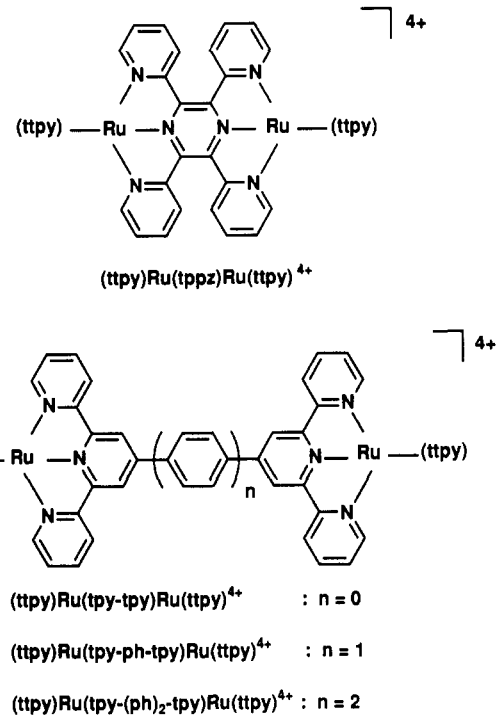

Figure 17. Rigidly-bridged dinuclear ruthenium complexes.

10. Synthesis of Rigidly-Bridged Homo- and Heterodinuclear Complexes

The homodivalent ruthenium precursor systems, depicted in Figure 17, were prepared in order to study mixed-valence complexes and to investigate electronic coupling within these compounds. Such complexes were obtained by heating $Ru(ttpy)L_3^{2+}$ (2 equiv) (L = acetone) and the bridging ligand (tppz, tpy-tpy, tpy-ph-tpy, or tpy-$(ph)_2$-tpy) in DMF for 3 h at 120 °C.[145] The compounds were purified by column chromatography on silica using CH_3CN–H_2O–*n*BuOH–aqueous KNO_3 mixtures of various proportions as eluent. All the compounds were isolated as their PF_6^- salts. The yields obtained were not always easy to reproduce. In average, they were as follows: (ttpy)Ru(tppz)Ru(ttpy)$^{4+}$ (52%), (ttpy)Ru(tpy-tpy)Ru(ttpy)$^{4+}$ (49%), (ttpy)Ru(tpy-ph-tpy)Ru(ttpy)$^{4+}$ (19%), and (ttpy)Ru(tpy-$(ph)_2$-tpy)Ru(ttpy)$^{4+}$ (35%).

All the compounds described in this section were characterized by ^1H NMR and FAB-MS. FAB-MS turned out to be particularly useful with these highly positively-charged species. In each case, the molecular

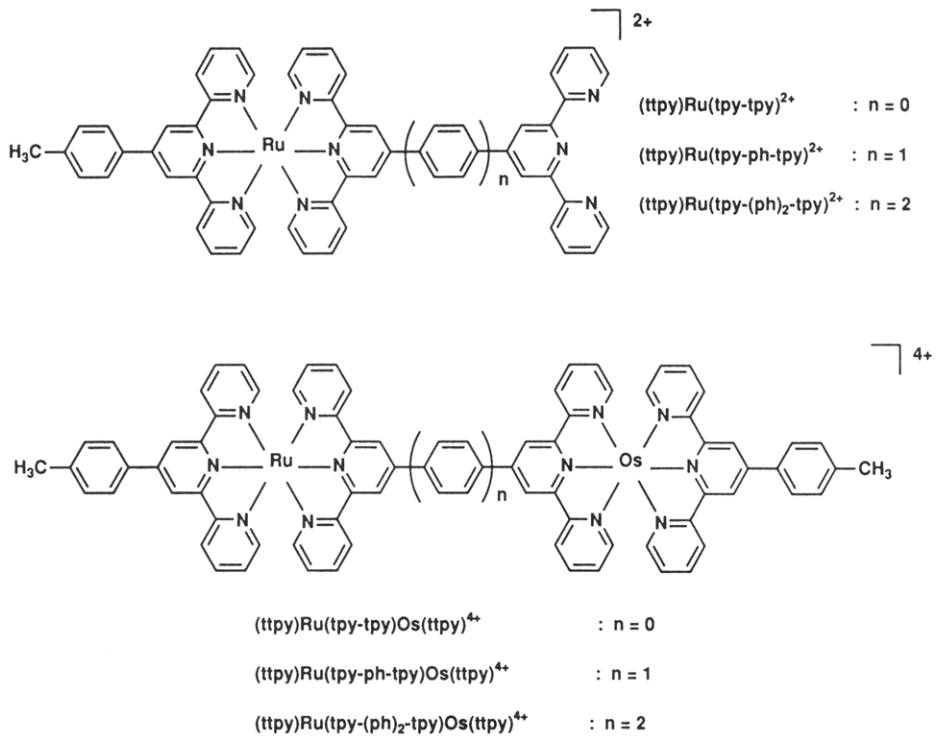

Figure 18. Mononuclear ruthenium precursors and rigidly-bridged ruthenium–osmium complexes.

peak was intense enough to exclude any ambiguity concerning the structure of the compound: (ttpy)Ru(tppz)Ru(ttpy)$^{4+}$ FAB-MS m/z = 763.8 ((ttpy)Ru(tppz)Ru(ttpy)$(PF_6)_3^+$ requires 763.6); (ttpy)Ru(tpy-tpy)Ru(ttpy)$^{4+}$ FAB-MS m/z = 1748.6 ((ttpy)Ru(tpy-tpy)Ru(ttpy)$(PF_6)_3^+$ requires 1748.4); (ttpy)Ru(tpy-ph-tpy)Ru(ttpy)$^{4+}$ FAB-MS m/z = 1825.1 ((ttpy)Ru(tpy-ph-tpy)Ru(ttpy)$(PF_6)_3^+$ requires 1824.5); (ttpy)Ru(tpy-(ph)$_2$-tpy)Ru(ttpy)$^{4+}$ FAB-MS m/z = 1902.4 ((ttpy)Ru(tpy-(ph)$_2$-tpy)Ru(ttpy)$(PF_6)_3^+$ requires 1901.0). Preparation of other complexes related to (ttpy)Ru(tppz)Ru(ttpy)$^{4+}$ and (ttpy)Ru(tpy-tpy)Ru(ttpy)$^{4+}$ has also been reported.[99,123,142,146]

By using the same bridging ligands as for the symmetrical diruthenium complexes (except tppz), heterocompounds were prepared with the aim of studying photoinduced energy- or electron-transfer processes between the two bridged complex subunits. As discussed in section 11.1, the Ru–Os system is particularly well adapted to energy transfer. The two different metals were complexes to the bridging ligand in a stepwise fashion, introducing first the ruthenium subunit followed by coordination of osmium. By inverting the order of complexation (osmium first), preparation of the heterodinuclear complexes is much less efficient. The intermediate mononuclear complexes and the final Os–Ru heterodinuclear compounds are represented in Figure 18. The mononuclear species (ttpy)Ru(tpy-tpy)$^{2+}$, (ttpy)Ru(tpy-ph-tpy)$^{2+}$, and (ttpy)Ru(tpy-(ph)$_2$-tpy)$^{2+}$ were prepared as follows. Ru(ttpy)Cl_3 and $AgBF_4$ were refluxed in acetone in order to remove the chlorine atoms from the metal. The complex obtained was added to a DMF solution of the bridging ligand and the mixture was refluxed (153 °C) for 1 h. After workup and chromatography on alumina with CH_3CN as eluent, the compound was isolated as its PF_6^- salt in good yield: (ttpy)Ru(tpy-tpy)$^{2+}$ (85%); (ttpy)Ru(tpy-ph-tpy)$^{2+}$ (77%); (ttpy)Ru(tpy-(ph)$_2$-tpy)$^{2+}$ (76%).

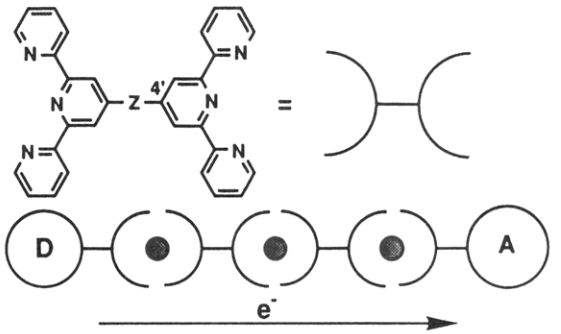

Figure 19. Multinuclear bis-tpy complexes end functionalized by electroactive groups for performing vectorial charge separation. The various bis-tpy complexes can be either photoactive components or simply electrophores. Z stands for any connecting unit.

The complexes (ttpy)Ru(tpy-tpy)Os(ttpy)$^{4+}$, (ttpy)Ru(tpy-ph-tpy)Os(ttpy)$^{4+}$, and (ttpy)Ru(tpy-(ph)$_2$-tpy)Os(ttpy)$^{4+}$ were then prepared by reaction of Os(ttpy)(Cl_3) with the corresponding Ru complex (ttpy)Ru(tpy-(ph)$_n$-tpy)$^{2+}$ in refluxing nBuOH for 7 h. All these compounds display ^{1}H NMR and FAB mass spectra in agreement with their postulated structures.

Recent work allowed the isolation of a trimetallic species containing *two* bridging ligands.[147] By using the rigidly-bridged compounds as building blocks, it should thus be possible to construct multinuclear one-dimensional arrays leading to vectorial long-range energy migration or electron transfer, as represented in Figure 19.

11. Energy- and Electron-Transfer Processes in Dinuclear Metal Complexes

As we have seen in section 10, linear bridging ligands can be obtained by linking two tpy ligands back-to-back via the 4′-position (Figure 19). Interposition of rigid spacers between the two tpy units leads to rodlike bridging ligands of variable length. Such ditopic ligands

Table 4. Luminescence Data[a,105]

	Os-based				Ru-based		
	λ_{max}, nm	τ, ns	I_{rel}[b] (λ_{ex} 650 nm)	I_{rel}[c] (λ_{ex} 500 nm)	λ_{max}, nm	τ, ns	I_{rel}[c] (λ_{ex} 500 nm)
$Os(ttpy)_2^{2+}$ [d]	734	230	100[e]	100[e]			
$Ru(ttpy)_2^{2+}$					640	0.95	100[f]
(ttpy)Ru(tpy-tpy)Os(ttpy)$^{4+}$	800	110	7	6		<0.020[g]	<5[h]
(ttpy)Ru(tpy-ph-tpy)Os(ttpy)$^{4+}$	746	190	70	71		<0.020[g]	<5[h]
(ttpy)Ru(tpy-(ph)$_2$-tpy)Os(ttpy)$^{4+}$	738	200	61	72		<0.020[g]	<5[h]

[a] Deaerated butyronitrile solution, room temperature. [b] Only the Os-based chromophoric unit is excited. [c] The Ru-based and Os-based units are excited in a ca. 1:1 ratio. [d] Reference 107. [e] $\Phi_{em} = 2.1 \times 10^{-2}$. [f] $\Phi_{em} = 3.2 \times 10^{-5}$. [g] The signal decay at 650 nm coincides with the excitation pulse. [h] The onset of the Os-based emission precludes a more precise evaluation.

can be used to obtain homo- and heteronuclear metal complexes of well-defined structure where the metal-to-metal distance can be modulated. Species containing two different luminescent metal centers (e.g. Ru(II)-based and Os(II)-based units) are particularly suitable for energy transfer studies (eqs 1, 2, and 5, with P=Ru(II)- and Q=Os(II)-based units). Partial oxidation of species containing two identical metal centers (e.g., two Ru(II)-based units) leads to mixed-valence [i.e., Ru(II)/Ru(III)] species where photoinduced and optical (intervalence) electron-transfer processes can be investigated (eqs 1–3, and eq 4, respectively, with P=Ru(II)- and Q=Ru(III)-based units).

11.1. Energy Transfer

The dimetallic compounds of general formulae (tpy)M(tppz)M(tpy)$^{4+}$ and (tppz)M(tppz)M(tppz)$^{4+}$ (M = Ru(II) or Os(II) and the trimetallic species (tpy)-Ru(tppz)Ru(tppz)Ru(tpy)$^{6+}$ have been prepared, and their electrochemical and spectroscopic properties have been investigated[108,109,148] together with those of the model mononuclear species. The differences observed in the metal-based oxidation potentials between metal centers in the homodimetallic complexes suggest noticeable metal–metal interactions through the bridging tppz ligand.[108,148] The MLCT transitions at lower energy involve the tppz ligand and move to the red in going from the mono- to the di- and trinuclear species. None of the oligonuclear species shows luminescence,[108] although the dinuclear compound (tpy)Ru(tppz)Ru-(tpy)$^{4+}$ was previously reported to exhibit a luminescence band at 826 nm (τ = 100 ns)[109] in acetonitrile at room temperature. The dimetallic (tpy)Ru(tppz)-$IrCl_3^{2+}$ compounds emits at 810 nm with τ = 22 ns (acetonitrile, room temperature) from a Ru-based ^{3}MLCT level.[149] Energy transfer from the Ir-based to the Ru-based moiety is efficient. In this compound, Ru(II)/Ru(III) and Ir(III)/Ir(IV) oxidations take place at +1.56 and +1.92 V (vs Ag/AgCl), respectively.[149]

The dinuclear complexes **5** and **6** which contain a $Ru(tpy)_2^{2+}$ chromophore, have been prepared, and their spectroscopic and electrochemical properties have been investigated.[150] The Ru–Ru complex **5** shows two distinct absorption bands, one at 480 nm corresponding to the $Ru(tpy)_2^{2+}$ unit and one at 967 nm due to the $Ru(bpy)_2(sq)^+$ unit (sq = the monoanionic semiquinone ligand arising from one-electron oxidation of catechol). Both bands are somewhat perturbed compared with those of the two independent components. In the Ru–Pd compound **6**, the ligand-to-ligand (catecholate → bipyridine) charge-transfer band is blue-shifted (524 *vs* 535 nm) and much more intense (ϵ = 19000 *vs* 1300 M^{-1} cm^{-1}) compared with the same band of the free

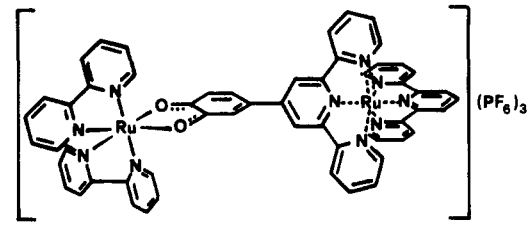

5

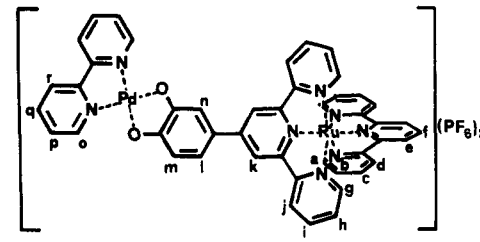

6

Pd(bpy)(cat) component (cat = dianion of catechol). The dinuclear compound is also reported to be a more efficient photosensitizer of singlet oxygen production than the mononuclear Pd complex.[150]

The absorption and luminescence properties of the compounds (ttpy)Ru(tpy-(ph)$_n$-tpy)Os(ttpy)$^{4+}$ (n = 0,1,2) shown in Figure 18 have been investigated to throw light on the electronic interaction through phenyl spacers.[105] The absorption spectra of the three binuclear compounds are shown in Figure 20, where the spectra of the two mononuclear model compounds $Ru(ttpy)_2^{2+}$ and $Os(ttpy)_2^{2+}$ are also displayed for comparison purposes. The ^{1}MLCT and ^{3}MLCT absorption bands of the dinuclear compounds move to lower energies along the series n = 2,1,0. The displacement from the spectrum of (ttpy)Ru(tpy-(ph)$_2$-tpy)Os(ttpy)$^{4+}$ is small for (ttpy)Ru(tpy-ph-tpy)Os(ttpy)$^{4+}$, but considerable for (ttpy)Ru(tpy-tpy)Os(ttpy)$^{4+}$. The luminescence data are collected in Table 4. In order to investigate the occurrence of energy transfer in the binuclear compounds, experiments were performed at two different excitation wavelengths. On excitation with 650-nm light, which is only absorbed by the Os-based component (Figure 20), the luminescence behaviors of (ttpy)Ru(tpy-(ph)$_2$-tpy)Os(ttpy)$^{4+}$ and (ttpy)-Ru(tpy-ph-tpy)Os(ttpy)$^{4+}$ are very similar (Figure 20 and Table 4). For (ttpy)Ru(tpy-tpy)Os(ttpy)$^{4+}$, however, a noticeable decrease in the energy and lifetime of the luminescent level as well as in the luminescence intensity is observed, indicating a rather strong inter-component interaction. When excitation is performed at 500 nm, where the Ru-based components of the binuclear compounds are excited in an approximately 1:1 ratio (Figure 20), the luminescence behavior is

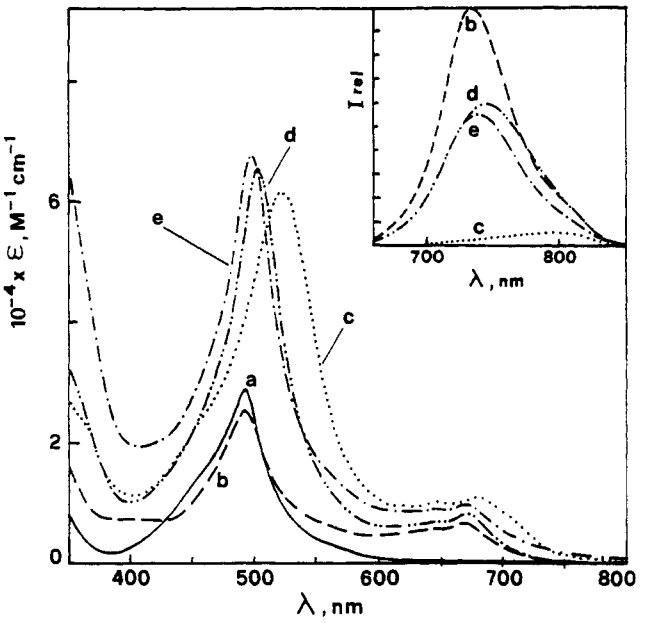

Figure 20. Absorption and (inset) luminescence spectra of (a)$Ru(ttpy)_2^{2+}$, (b) $Os(ttpy)_2^{2+}$, (c) (ttpy)Ru(tpy-tpy)Os(ttpy)$^{4+}$, (d) (ttpy)Ru(tpy-ph-tpy)Os(ttpy)$^{4+}$, and (e) (ttpy)-Ru(tpy-$(ph)_2$-tpy)Os(ttpy)$^{4+}$.

practically identical to that observed upon 650-nm excitation (Table 4). In particular, for each compound the shape of the luminescence band is exactly the same as that of the band obtained upon 650-nm excitation, where only the Os-based component can be excited. This finding suggests that the luminescent excited state of the Ru-based component is completely quenched in the binuclear species. Picosecond experiments have confirmed this finding and have established an upper limit of 20 ps for the lifetime of the Ru-based excited state in the binuclear species.[105]

The results obtained indicate that the strong electronic interaction observed between the two components in (ttpy)Ru(tpy-tpy)Os(ttpy)$^{4+}$ is substantially reduced upon interposition of a phenyl spacer. A second phenyl spacer causes a further, but small, reduction of the interaction. In fact, the absorption and Os-based luminescence properties of (ttpy)Ru(tpy-$(ph)_2$-tpy)Os(ttpy)$^{4+}$ are only slightly different from those of a 1:1 mixture of $Ru(ttpy)_2^{2+}$ and $Os(ttpy)_2^{2+}$ (Table 4), which may be considered as an approximate model of a supramolecular system where the Ru-based and Os-based components do not interact. The electronic energy-transfer process from the Ru-based to the Os-based component, however, is 100% efficient and takes place with a rate constant higher than 5×10^{10} s^{-1} even when the two components are separated by two phenyl rings (metal-to-metal distance, 20 Å).

11.2. Intervalence Transfer

As mentioned above, dinuclear homometallic rod-like compounds are very suitable for investigations concerning intervalence transfer processes. Oxidation of (ttpy)Ru(tppz)Ru(ttpy)$^{4+}$ and (ttpy)Ru(tpy-$(ph)_n$-tpy)Ru(ttpy)$^{4+}$ (Figure 17) leads to the corresponding mixed-valence Ru(II),(III) species.[148] From CPK molecular models, the metal-to-metal separation distance in these four compounds is estimated to be 7, 11, 15.5, and 20 Å, respectively. In the case of (ttpy)Ru(tppz)-Ru(ttpy)$^{4+}$ the oxidation potential of the two equivalent metal centers differs by as much as 0.3 V, indicating a strong communication through the bridging ligand. The mixed-valence (ttpy)Ru(tppz)Ru(ttpy)$^{5+}$ compound shows an intervalence transfer band with maximum at 1520 nm, from which an interaction energy of 0.4 eV (half the band energy) can be estimated in the assumption that the compound can be classified as a class III species (section 4.2). For the phenyl-separated species (ttpy)Ru(tpy-$(ph)_n$-tpy)Ru(ttpy)$^{4+}$, the interaction energy is much smaller, as can be inferred by the lack of two distinct oxidation waves. A relatively weak interaction has also been observed for $Ru(NH_3)_5py^{2+}$ centers separated by phenyl rings.[134] Titration with Ce(IV) of (ttpy)Ru(tpy-$(ph)_n$-tpy)Ru(ttpy)$^{4+}$ causes[148] (i) a decrease in the intensity of the MLCT absorption band, (ii) the increase in the intensity of the LMCT band characteristic of Ru(III) complexes, and (iii) a rise and decay of the intensity of the infrared intervalence-transfer band (Table 5). From the latter variation, comproportionation constants were found near the statistical limit. This allowed the calculation of the corrected spectra of the mixed-valence species. By using the parameters of the intervalence-transfer band, the values of the interaction energy were obtained (Table 5). As expected, the interaction energy decreases with increasing number of phenyl spacers. Comparison with the results obtained with dinuclear Ru(II,III) species separated by polyene bridges[63,151] suggests that the decreasing effect on the interaction energy caused by a phenyl ring is equal to that caused by two double bonds. Polyphenylated bridges can therefore replace the synthetically less accessible and chemically more fragile polyene systems in a variety of photochemical molecular devices.

When two dpbH (7) cyclometalating ligands are linked back-to-back, the bis-cyclometalating 3,3′,5,5′-tetrapyridylbiphenyl bridging ligand, tpbp-H_2 (8), is obtained. In its dinuclear cyclometalated mixed-valence compounds (ttpy)M^{II}(tpbp)M^{III}(ttpy)$^{3+}$ (9, M = Ru or Os), very intense intervalence bands are observed[152,153] (λ_{max} = 1820 nm, ϵ = 27 000 M^{-1} cm^{-1} for the Ru complex). This result can be explained by the covalent character of the C^-–metal bond and the consequent electron delocalization.

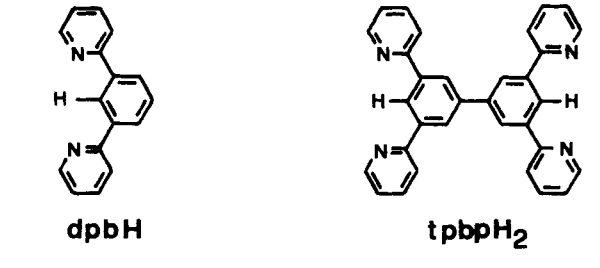

dpbH

7

$tpbpH_2$

8

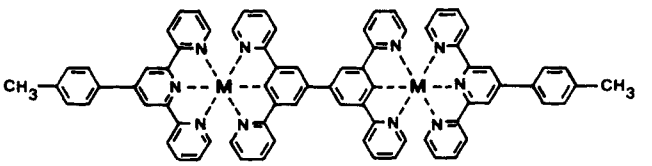

$[(ttpy)M^{II}(tpbp)M^{III}(ttpy)]^{3+}$ M = Ru or Os

9

Table 5. Intervalence Band Parameters and Derived Electronic Coupling H for the Ru^{II}–Ru^{III} Complexes[a,148]

complex	λ_{max}, nm	ϵ_{max}, M^{-1} cm^{-1}	$\Delta\nu_{1/2}$, cm^{-1}	r, Å	H, eV
(ttpy)Ru(tpy-tpy)Ru(ttpy)$^{5+}$	1580	1618	4008	11	0.047
(ttpy)Ru(tpy-ph-tpy)Ru(ttpy)$^{5+}$	1295	729	6036	15.5	0.030
(ttpy)Ru(tpy-(ph)$_2$-tpy)Ru(ttpy)$^{5+}$	1150	709	4934	20	0.022

[a] CH_3CN solution, room temperature.

Table 6. Electrochemical Potentials and Their Assignments[a,106,107,112,127]

	$M^{3+/2+}$	$DPAA^{+/0}$	$PTZ^{+/0}$	$MV^{2+/+}$	$ttpy^{0/-}$ [b]
$Ru(ttpy)_2^{2+}$	+1.25				−1.24
$Ru(ttpy)_2^{2+}$–MV^{2+}	+1.27			−0.36	−1.21
PTZ–$Ru(ttpy)_2^{2+}$	+1.27		+0.79		−1.23
DPAA–$Ru(ttpy)_2^{2+}$	+1.27	+0.77			−1.26
PTZ–$Ru(ttpy)_2$-MV^{2+}	+1.25		+0.76	−0.39	−1.24
DPAA–$Ru(ttpy)_2$-MV^{2+}	+1.26	+0.75		−0.40	−1.26
$Os(ttpy)_2^{2+}$	+0.89				−1.17
$Os(ttpy)_2^{2+}$–MV^{2+}	+0.90			−0.35	−1.20
PTZ–$Os(ttpy)_2$	+0.90		+0.76		−1.19
DPAA–$Os(ttpy)_2^{2+}$	+0.94	+0.76			−1.24
PTZ–$Os(ttpy)_2^{2+}$–MV^{2+}	+0.94		+0.78	−0.37	−1.17
DPAA–$Os(ttpy)_2$–MV^{2+}	+0.94	+0.75		−0.48	−1.21
MV^{2+} [c]				−0.44	
MePTZ[d]			+0.74		
MeDPAA[e]		+0.65			

[a] Acetonitrile solution, 298 K; $E_{1/2}$ values in volts, vs SSCE. For nomenclature problems see text. [b] The reduction wave of the second ttpy ligand occurs at more negative potentials. [c] $E_{1/2}$ = −0.40 V vs Ag/AgCl; the reduction potential for the ttpy-MV^{2+} moiety is −0.36 V. [d] $E_{1/2}$ = +0.40 V vs Ag/Ag^+; th reduction potential for the ttpy-PTZ^+ moiety is +0.79 V. [e] Methyldi(-*p*-anisyl)amine; the reduction potential for the ttpy-$DPAA^+$ moiety is +0.74 V.

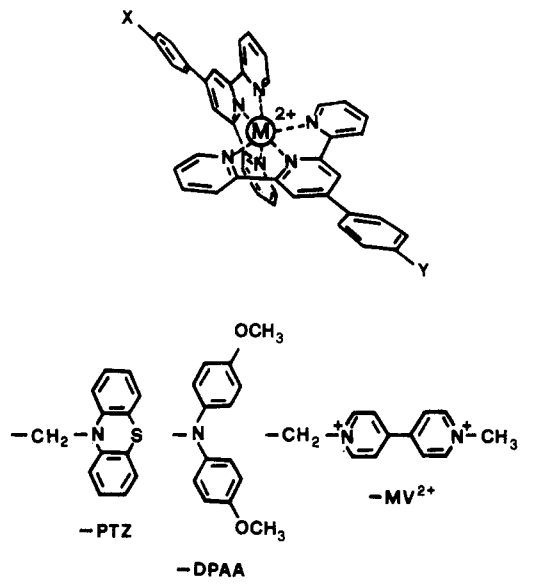

Figure 21. Schematic view and composition of the dyads and triads. X and Y groups can be the indicated -PTZ, -DPAA, and -MV^{2+} groups.

12. Photoinduced Charge Separation in Dyads and Triads

Photoinduced charge-separation processes have been investigated in P–A and D–P dyads and in D–P–A triads where the photosensitizer P is $M(ttpy)_2^{2+}$ (M = Ru(II) or Os(II), Figure 21).[106,107,112,154] In looking at the scheme and at the formulae for the supramolecular species used hereafter it should be taken into account that in covalently-linked multicomponent systems there are nomenclature problems related to the fact that covalent linking implies more or less small modifications of the isolated molecular species. For example, 4′-(*p*-tolyl)-2,2′:6′,2″-terpyridine and its abbreviation ttpy are right when used for the ligands of the isolated photosensitizer $Ru(ttpy)_2^{2+}$, but are not corret when applied to the photosensitizer component of dyads or triads. It is however preferable to maintain the same abbreviations (see Table 6–9) for the free and covalently-linked components in order to better understand the chemical parentage of the various systems investigated. Other problems related to the actual nature of the photosensitizer and to intercomponent interactions will be discussed below.

12.1. Electrochemical Properties

The electrochemical properties of the investigated dyads and triads and of their isolated components are summarized in Table 6.[107,112] The reversible oxidation wave at +1.25 V for $Ru(ttpy)_2^{2+}$ and +0.89 V for $Os(ttpy)_2^{2+}$ can be assigned to a metal-centered process. The first reduction wave at −1.24 and −1.17 V for $Ru(ttpy)_2^{2+}$ and $Os(ttpy)_2^{2+}$, respectively, can be assigned to the one-electron reduction of a ttpy ligand. The well-known reduction wave of MV^{2+} is reversible, as is also the case for the first oxidation wave of PTZ and MeDPAA (which may be considered as a reference compound for –DPAA). The reduction of the second ttpy ligand, the second reduction of MV^{2+}, and the second oxidations of PTZ and MeDPAA are also known but they are not relevant to the following discussion. The electrochemical waves of the dyads and triads can easily be assigned by comparison with the waves observed for the isolated components. It can be noticed, however, that in several cases there are nonnegligible differences between the potential values of the same components in different supramolecular species. For example, MV^{2+} is easier to reduce in the dyad than in the triads involving DPAA (Table 6). The cyclic voltammogram for the $[PTZ\text{-}Ru(ttpy)_2^{2+}\text{-}MV^{2+}]^{4+}$ triad is presented in Figure 22. The energies of the various charge-separated states in the examined dyads and

Table 7. Absorption Maxima[a,106,107,112,127]

	λ_{max}, nm (ϵ, M^{-1} cm^{-1})			
$Ru(ttpy)_2^{2+}$	284 (68 000)	310 (76 000)	490 (28 000)	
$Ru(ttpy)_2^{2+}$–MV^{2+}	285 (98 000)	311 (79 000)	491 (32 000)	
PTZ–$Ru(ttpy)_2^{2+}$	285 (75 000)	310 (84 000)	490 (31 000)	
DPAA–$Ru(ttpy)_2^{2+}$	284 (63 000)	310 (81 000)	502 (39 000)	
PTZ–$Ru(ttpy)_2^{2+}$-MV^{2+}	285 (112 000)	310 (83 000)	491 (32 000)	
DPAA–$Ru(ttpy)_2^{2+}$-MV^{2+}	283 (83 000)	310 (77 000)	504 (43 000)	
$Os(ttpy)_2^{2+}$	286 (58 000)	314 (68 000)	490 (26 000)	667 (6 600)
$Os(ttpy)_2^{2+}$–MV^{2+}	285 (68 000)	315 (61 000)	490 (23 000)	668 (5 700)
PTZ–$Os(ttpy)_2^{2+}$	286 (68 000)	314 (75 000)	490 (28 000)	668 (7 100)
DPAA–$Os(ttpy)_2^{2+}$	285 (53 000)	314 (70 000)	503 (31 000)	671 (7 800)
PTZ–$Os(ttpy)_2^{2+}$–MV^{2+}	287 (66 000)	315 (56 900)	491 (24 000)	669 (6 700)
DPAA–$Os(ttpy)_2^{2+}$–MV^{2+}	280 (81 000)	314 (79 000)	504 (40 000)	672 (9 200)
MV^{2+} [b]	260 (20 400)			
MV^{+} [b]		397 (41 800)		607 (13 900)
$MeDPAA^{+}$ [c]		395 (14 000)	570 (48 00)	740 (26 600)

[a] Acetonitrile solution, room temperature. [b] Reference 155. [c] In CH_2Cl_2 solutions, ref 140b.

Table 8. Luminescence Data[a,107,112]

	155 K			298 K		
	λ_{max}, nm	τ, ns	I_{rel}[b]	λ_{max}, nm	τ, ns	I_{rel}[b]
$Ru(ttpy)_2^{2+}$	648	800	100			
$Ru(ttpy)_2^{2+}$–MV^{2+}	661	15	2			
DPAA–$Ru(ttpy)_2^{2+}$	678	600	105			
DPAA–$Ru(ttpy)_2^{2+}$–MV^{2+}	675	15	2			
$Os(ttpy)_2^{2+}$	740	540	100	734	220	100
$Os(ttpy)_2^{2+}$–MV^{2+}	745	4	1.9	738	0.26	1.2
DPAA–$Os(ttpy)_2^{2+}$	749	490	78	743	190	75
DPAA–$Os(ttpy)_2^{2+}$–MV^{2+}	755	1.5	~1	747	0.19	~1

[a] Butyronitrile solvent. [b] Arbitrary value, taken as a reference for the compounds of the same family under the same experimental conditions.

Table 9. Approximate Values for the Energies of the Excited States[a,107,112]

	*P	P^+–A^-	D^+–P^-	D^+–P–A^-
$Ru(ttpy)_2^{2+}$	1.96			
$Ru(ttpy)_2^{2+}$–MV^{2+}	1.96	1.63		
PTZ–$Ru(ttpy)_2^{2+}$	1.96		2.06	
DPAA–$Ru(ttpy)_2^{2+}$	1.89		2.04	
PTZ–$Ru(ttpy)_2^{2+}$–MV^{2+}	1.96	1.64	2.00	1.15
DPAA–$Ru(ttpy)_2^{2+}$–MV^{2+}	1.89	1.66	2.01	1.15
$Os(ttpy)_2^{2+}$	1.69			
$Os(ttpy)_2^{2+}$–MV^{2+}	1.69	1.25		
PTZ–$Os(ttpy)_2^{2+}$	1.69		1.95	
DPAA–$Os(ttpy)_2^{2+}$	1.66		1.95	
PTZ–$Os(ttpy)_2^{2+}$–MV^{2+}	1.69	1.31	1.95	1.15
DPAA–$Os(ttpy)_2^{2+}$–MV^{2+}	1.66	1.42	1.96	1.23

[a] Energy in electron volts; acetonitrile or butyronitrile solutions.

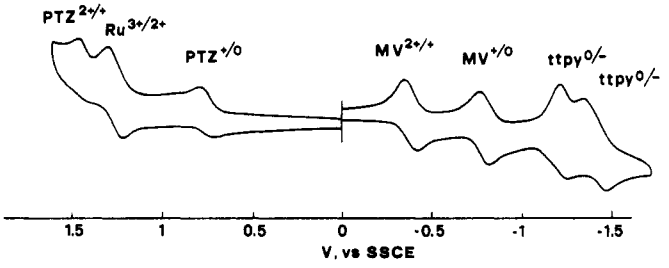

Figure 22. Cyclic voltammogram for the PTZ–$Ru(ttpy)_2^{2+}$–MV^{2+} triad.

triads can be estimated from the data of Table 6. The values so obtained, however, are not the exact energy values of the various levels in the photochemical experiments because of the different solvent and temperature conditions (vide infra).

12.2. Ground-State Absorption Spectra

The absorption spectra of $Ru(ttpy)_2^{2+}$ and $Os(ttpy)_2^{2+}$ are characterized by the well-known LC bands in the UV region and MLCT bands in the visible (Table 7).[107,112] Comparison of the spectroscopic properties for $Ru(tpy)_2^{2+}$ (Table 1) and $Ru(ttpy)_2^{2+}$ indicates a small red shift and a substantially larger molar absorption coefficient for the latter compound, thus confirming that light absorption actually leads to electron promotion to a ligand system that, to a certain degree, includes the tolyl fragment. Similar conclusions were reached by studying the influence of geometrical restraints and of electron-withdrawing and electron-repelling groups attached to remote positions of ttpy on the intensity of the absorption bands.[156] This supports the component subdivision of the reported supramolecular systems which is based on $M(ttpy)_2^{2+}$ as a photosensitizer (for more details, see below).

The electron-donor and -acceptor components of dyads and triads do not absorb in the visible region. Inspection of Table 7 reveals that the energy and the intensity of the MLCT bands of the photosensitizer are practically unaffected by the attached MV^{2+} and PTZ groups. When D = DPAA, however, the energy and intensity of the ^{1}MLCT band (and ^{3}MLCT band for the Os complex) show some change with respect to the isolated photosensitizer and the other systems. The room-temperature absorption spectra of $Os(ttpy)_2^{2+}$, $Os(ttpy)_2^{2+}$-MV^{2+}, and DPAA-$Os(ttpy)_2^{2+}$-MV^{2+} are shown in Figure 23.[112] The absorption maxima of MV^{+} [155,157] and $MeDPAA^{+}$,[140b] which are useful for the discussion of photoinduced electron-transfer processes, are also reported in Table 7.

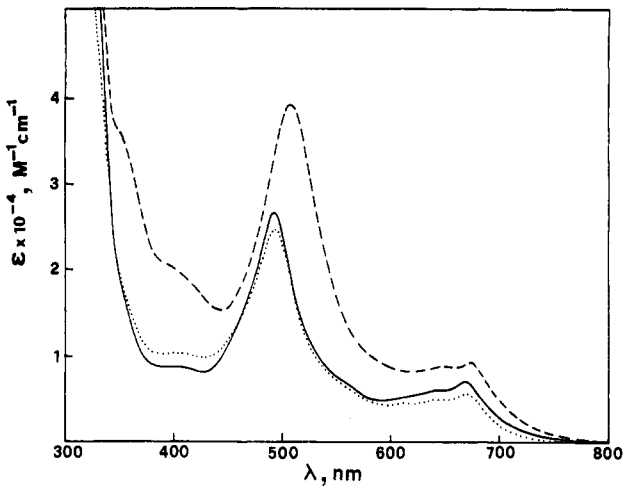

Figure 23. Absorption spectra of $Os(ttpy)_2^{2+}$ (solid line), $Os(ttpy)_2^{2+}$–MV^{2+} (dotted line), and DPAA–$Os(ttpy)_2^{2+}$–MV^{2+} (dashed line).

12.3. Luminescence Properties

The luminescent properties of photosensitizers, dyads, and triads are gathered in Table 8. Since $Ru(ttpy)_2^{2+}$ practically does not emit at room temperature, the experiments on this species and on its derivatives were performed at 155 K. For the compounds based on $Os(ttpy)_2^{2+}$, which is luminescent at room temperature, experiments were performed both at 155 and 298 K. The solvent used was butyronitrile. It can be noticed that the maximum of the luminescence band of the photosensitizer is somewhat red-shifted in the dyads and triads containing DPAA. It should also be pointed out that some experiments originally performed on the Ru-based compounds[107] in propionitrile–butyronitrile mixtures could not be reproduced. After accurate analyses, it was found[158] that impurities contained in butyronitrile and, especially, in propionitrile can cause the detachment of the electron acceptor from the photosensitizer in the dyads and triads by an unclear mechanism, leading to $Ru(ttpy)_2^{2+}$-type species that exhibit an "unquenchable" luminescence. For this reason, some of the conclusions drawn in the above mentioned paper[107] should be replaced with those reported here.

12.4. Mechanisms of the Photoinduced Processes

12.4.1. Systems Containing DPAA and/or MV^{2+}

Table 9 shows approximate values for the energies of the excited photosensitizers in the various supramolecular species (obtained from the maxima of the luminescence band at 90 K) and for the energies of the charge-separated states (obtained from the potentials shown in Table 6 and, when necessary, from the excited-state energies). Such values have to be considered as estimates rather than actual values, because of (i) the different conditions in which the electrochemical and spectroscopic data have been obtained and (ii) the different stabilization and Coulombic terms for the one-electron oxidized or reduced component and the charge-separated species.[159] It should also be noticed that MV^{2+}, PTZ, and DPAA do not exhibit low-energy electronic excited states, so that in the dyads and triads energy-transfer quenching cannot occur. Schematic energy level diagrams for the P–A dyads, and the D–P–A triads are shown in Figures 24 and 25. The energy-level diagrams for the D–P dyads are not shown since it is clear from the data reported in Table 9 that the electron-transfer reduction of *P by PTZ or DPAA is endoergonic and therefore it cannot compete with the intrinsic decay rate of the photosensitizer.

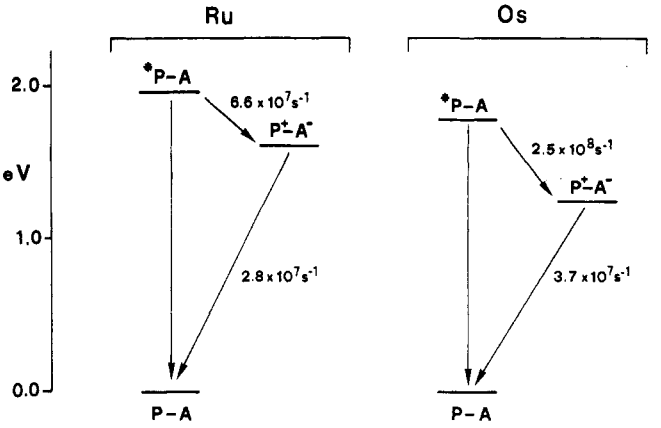

Figure 24. Photoinduced processes in the P–MV^{2+} dyads where P is $Ru(ttpy)_2^{2+}$ or $Os(ttpy)_2^{2+}$ at 155 K. For more details see text.

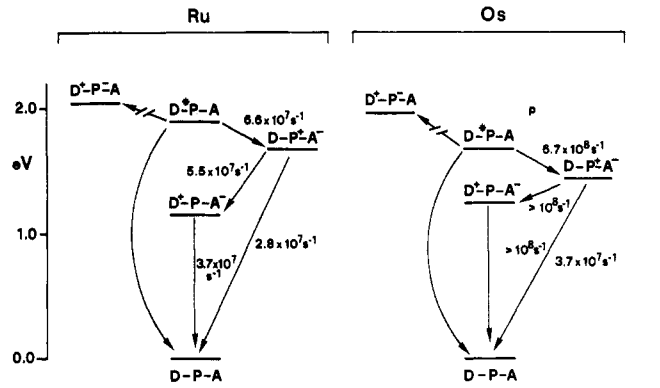

Figure 25. Photoinduced processes in the DPAA–P–MV^{2+} triads where P is $Ru(ttpy)_2^{2+}$ or $Os(ttpy)_2^{2+}$ at 155 K. For more details see text.

As it usually happens for ruthenium(II) and osmium(II) polypyridine complexes, light excitation in the spin-allowed MLCT bands eventually leads to the population of the lowest energy ^{3}MLCT level,[86] which is the state responsible for the observed electron-transfer processes (Figure 5).

In an attempt to compare the behavior of analogous Ru-based and Os-based systems, most of the following discussion will refer to the results obtained at 155 K. The isolated photosensitizers $Ru(ttpy)_2^{2+}$ and $Os(ttpy)_2^{2+}$ show transient absorption spectra characterized by the bleaching of the visible band at 490 nm and by positive absorptions around 400 and 600 nm. The latter two bands can be interpreted in terms of localization of the excited electron on one of the two equivalent ttpy ligands.[157,160] At 155 K the transient spectra decay with τ = 800 and 540 ns, respectively, which coincide with the luminescence lifetimes, indicating that the changes in absorbance are due to the formation and subsequent disappearance of the luminescent ^{3}MLCT excited state.

The behavior of the D–P dyads with D = PTZ is the same as that of the isolated photosensitizer, as it could

be expected because the D^+–P^- energy level lies at higher energy than that of *P (Table 9). Such an energy-level situation holds true also for D = DPAA. The small effects caused by DPAA on the luminescence intensity and lifetimes of *P (Table 8) can be attributed to perturbations of the ^{3}MLCT level of the photosensitizer induced by the conjugation with DPAA. Perturbation effects can also be observed, in fact, in the electrochemical behavior and the absorption spectra (*vide supra*). For the P–A dyads (A = MV^{2+}), the charge separated P^+–A^- level lies much below the ^{3}MLCT level P (0.33 eV for P = $Ru(ttpy)_2^{2+}$; 0.44 eV for P = $Os(ttpy)_2^{2+}$, Figure 24). A quenching of the photosensitizer luminescence via the charge-separated state can thus be expected. The results obtained (Table 8) show that for the Ru-based P–A dyad the lifetime of *P is reduced to 15 ns. A parallel quenching of the luminescence intensity is also observed. From the equation

$$k = \frac{1}{\tau} - \frac{1}{\tau^\circ} \qquad (26)$$

where τ and τ° are the luminescence lifetimes of *P–A and *P, respectively, a value of 6.6×10^7 s^{-1} can be obtained for the electron-transfer quenching process. The transient spectrum of the P^+–A^- charge-separated state of the dyad is very similar to that of the excited photosensitizer; the only sizeable difference concerns the amount of bleaching at 490 nm. This does not compromise the elucidation of the reaction kinetics since the rate of the quenching reaction can be obtained by luminescence measurements (*vide supra*) and the rate of the back-electron-transfer reaction can be measured by the decay of the transient spectrum ($k = 2.8 \times 10^7$ s^{-1}). The Os-based P–A dyad behaves qualitatively as the Ru-based one, with rate constants 2.5×10^8 s^{-1} for the excited-state quenching reaction and 3.7×10^7 s^{-1} for the back-electron-transfer reaction (Figure 24).

For the Ru-based D–P–A triad (Figure 25; D = DPAA; A = MV^{2+}), the luminescence decay is 15 ns as in the corresponding P–A dyad.[107,158] The transient spectrum obtained at τ = 20 ns is noticeably different from that obtained upon excitation of P and P–A. Besides a displacement of the bleaching to 505 nm (expected because of the perturbation caused by DPAA on the absorption spectrum of P, Table 7), positive absorption bands are present at 750 and 400 nm, assigned to the $DPAA^+$ radical cation (Table 7). The electron-transfer quenching reaction ($k = 6.6 \times 10^7$ s^{-1}) is thus followed, at least in part, by a fast secondary electron-transfer process which leads to the fully charge-separated state D^+–P–A^-. The rate of formation of D^+–P–A^- from D–P^+–A^- can be estimated from the formation lifetime of D^+ measured at 750 and 450 nm (ca. 18 ns, $k = \sim 5.5 \times 10^7$ s^{-1}). The decay of the D^+ absorption bands occurs with τ = 27 ns ($k = 3.7 \times 10^7$ s^{-1}) which can be assigned to the decay of D^+–P–A^- to the ground state D–P–A (Figure 25).

For the Os-based triad (Figure 25),[112] the electron-transfer quenching process leading to D–P^+–A^- takes place with $k = 6.7 \times 10^8$ s^{-1} (from the emission lifetime). Since no transient absorption or bleaching can be seen within the time resolution of the system used, one can conclude that the deactivation of D–P^+–A^- via the fully charge-separated state D^+–P–A^- occurs with $k > 10^8$ s^{-1}, i.e. it is faster than the rate of the back-electron-transfer process in the dyad ($k = 3.7 \times 10^7$ s^{-1}). The D^+–P–A^- spectrum is not detected, because this species does not accumulate and it rapidly deactivates to D–P–A.

For the Os-based compounds, experiments have also been performed at room temperature.[112] In butyronitrile solution, the 220-ns luminescence lifetime of $Os(ttpy)_2^{2+}$ is reduced to 260 ps in the P–A dyad (A = MV^{2+}) and to 190 ps in the D–P–A triad (D = DPAA; A = MV^{2+}). The rate constant for the electron-transfer quenching process is therefore of the order of 5×10^9 s^{-1}. No transient absorption spectrum could be observed, indicating that the decay of the charge-separated state takes place within the instrumental resolution time ($k > 10^8$ s^{-1}). In ethanol solution at room temperature the luminescence lifetime of the Os-based photosensitizer (240 ns) is reduced to 720 ps in the P–A dyad (rate constant of the electron-transfer quenching reaction, 1.4×10^9 s^{-1}).[154] In butyronitrile rigid matrix at 90 K the luminescence lifetime is the same for *P and *P–A,[112] indicating that the electron-transfer quenching process cannot take place under these conditions.

An analysis of the above results in the light of current electron-transfer theories (section 4.1) is difficult for several reasons. First of all, in the above described multicomponent systems the photosensitizer is, in principle, a multicomponent system by itself since (i) its reactive excited state is MLCT in nature, and (ii) its oxidation and reduction processes are metal and ligand centered, respectively. In reality, the metal–ligand bonds exhibit a nonnegligible covalent character, whose degree depends on the nature of the metal and on the oxidation state of metal and ligand. A further element of difficulty arises from the fact that, at least in some cases (Tables 6–8), there is a nonnegligible interaction between the components of the dyads and triads. For these reasons the exact amount and localization of the transferred charge in the formally one-electron transfer elementary steps is not known. As a consequence, an appropriate use of eq 10 to calculate the outer-sphere reorganizational energy is prevented.[65,66] This is a very common (but often overlooked) problem in the analysis of photoinduced electron-transfer processes in multicomponent systems involving transition metal complexes. The inner-sphere reorganization energy (which is a much less important term) is also difficult to estimate because of the above-mentioned charge delocalization and the presence of groups, like DPAA, which could exhibit very different geometries depending on the oxidation state. Further problems arise because the free-energy change of the various electron-transfer processes in butyronitrile solution at 155 K is not the same as that available from electrochemical measurements in acetonitrile solution at room temperature. Because of these difficulties, we will only make a few comments on the rates of the photoinduced processes in the P–A and D–P–A systems.

The photoinduced electron-transfer process *P–A → P^+–A^- is most likely adiabatic since the photosensitizer is directly linked to, or separated by a phenyl spacer (depending on whether P is taken to be $M(tpy)_2^{2+}$ or $M(ttpy)_2^{2+}$) from the electron acceptor. On this assumption, the experimental rate constants (6.6×10^7

Table 10. Absorption Data of Ferrocene-Containing Complexes[a,140]

complex	λ_{max}, nm (ϵ_{max}, M^{-1} cm^{-1})					
Fc	326 (50)	442 (90)				
Fc-phtpy	254 (13 300)	287 (18 900)	369 (2 100)	451 (1 220)[b]		
$Ru(Fc\text{-}phtpy)_2^{2+}$	233 (48 500)	275 (46 700)	283 (46 400)	312 (75 100)	330 (67 900)	501 (34 800)
$Os(Fc\text{-}phtpy)_2^{2+}$	275 (43 800)	292 (39 800)	316 (66 500)	501 (29 200)	672 (8 400)	
$(Fc\text{-}phtpy)Ru(ttpy)^{2+}$	284 (48 500)	311 (62 200)	495 (26 000)			
$(Fc\text{-}phtpy)Os(ttpy)^{2+}$	286 (40 300)	315 (54 100)	495 (20 300)	670 (5 35)		

[a] All data taken at room temperature in CH_3CN solution except as indicated. [b] In CH_2Cl_2.

s^{-1} for the Ru-based dyad and 2.5×10^8 s^{-1} for the Os-based one) and the $\Delta G°$ values (−0.33 and −0.44 eV, respectively) lead to a λ value of ~1.1–1.3 eV. Taking $\lambda_i \simeq 0.2$ eV, λ_o results to be ~0.9–1.1 eV. However, on the assumption of the transfer of a full electron over 12.3 Å (the center-to-center $M(ttpy)_2^{2+}$–MV^{2+} distance), a λ_o value of 1.7 eV would be obtained by using eq 10. This discrepancy emphasizes the above mentioned difficulties concerning the amount and localization of the transferred charge.

The back-electron-transfer reactions in the dyads are noticeably exoergonic (−1.63 and −1.25 eV in the Ru- and Os-based compounds, respectively). They could therefore be expected to lie in the Marcus inverted region. On the assumption of an adiabatic behavior, from the experimental rate constants and the free energy changes, λ values of 0.92 and 0.66 would be obtained. Such values are much smaller than the above-calculated value (λ = 1.7 eV). This shows again that the assumptions on which eq 10 is based are not realistic in these systems. It should also be noted that the back-electron-transfer reaction could exhibit some degree of nonadiabaticity.

For the D^+–P–A^- → D–P–A back-electron-transfer reaction, eq 10 yields a value of 2.2 eV for λ_o on the assumption of the transfer of a full electron over the center-to-center separation distance (23 Å). This would yield a value of ~2.4 eV for λ. Since $\Delta G°$ is −1.15 and −1.23 eV for the Ru- and Os-based system, respectively, the process should be strongly activated, with rate constants ~5×10^6 and 2×10^7 s^{-1}, respectively, i.e. lower than the experimental values, even in the unlikely case of an adiabatic regime. This discrepancy points out once again that simple relationships do not hold for these systems.

In general, it should be noticed that in polar solvents the outer-sphere reorganizational energy for electron transfer over long distances is very large. For example, in acetonitrile solution at room temperature λ_o (as calculated by eq 10) is 1.28 eV for r = 12 Å and 1.7 eV for r = 23 Å. Therefore, for triads based on Ru(II) and Os(II) photosensitizers ($E^{0\text{-}0}$ of the reactive excited state ~1.5–2.0 eV) it is difficult to place the back-electron-transfer reaction of the fully charge separated excited state, obtained by two successive exoergonic processes, in the Marcus inverted region. High-energy, long-lived charge-separated states could in principle be obtained by an appropriate design of the electronic factor. Long lived low energy charge-separated states can of course be obtained by virtue of the high activation energy of the back electron transfer process. In low polarity solvents, of course, the situation changes drastically. For CH_2Cl_2 (ϵ_s = 9.1) and cyclohexane (ϵ_s = 2.28), eq 10 yields λ_o values of 1.2 and 0.02 eV, respectively, for a center-to-center distance of 23 Å. In very low polarity solvents, however, transition metal complexes are often poorly soluble.

Table 11. Electrochemical Data of Ferrocene-Containing Complexes[a,140]

complex	redox potentials, V (ΔE_p, mV)[a]			
	$M^{3+/2+}$	$Fc^{+/0}$	$L^{0/-}$	$L^{-/2-}$
Fc		+0.50 (95)		
Fc-phtpy		+0.56 (80)		
$Ru(Fc\text{-}phtpy)_2^{2+}$	+1.42 (i)	+0.56 (80)	−1.17 (75)	−1.41 (70)
$Os(Fc\text{-}phtpy)_2^{2+}$	+1.05 (i)	+0.57 (70)	−1.15 (70)	−1.37 (170)
$(Fc\text{-}phtpy)Ru(ttpy)^{2+}$	+1.30 (i)	+0.57 (90)	−1.17 (75)	−1.41 (70)
$(Fc\text{-}phtpy)Os(ttpy)^{2+}$	+0.98 (i)	+0.57 (85)	−1.13 (65)	−1.38 (85)

[a] Unless otherwise stated, potentials are quoted vs SSCE in DMF at a Pt electrode; (i) = irreversible. Supporting electrolyte is NEt_4ClO_4.

12.4.2. Systems Containing Ferrocene

Ferrocene is a useful redox agent as it is easily oxidized and exhibits a reversible behavior in many solvents (Fc^+/Fc = +0.50 V vs SSCE in DMF[140]). These properties make ferrocene a largely employed reference system in electrochemical experiments. Because of its facility to be oxidized, ferrocene is expected to act as an electron donor in multicomponent systems designed for the study of charge-separation processes. Recent reports are in fact concerned with chelating ligands linked to a ferrocene unit.[140,161]

As discussed in section 7.1, the tpy ligands are suitable fragments for bearing appended groups on the 4′ position. Therefore systems of the type D–P (dyads) and D–P–A (triads), where P is the $Ru(ttpy)(phtpy)^{2+}$- or $Os(ttpy)(phtpy)^{2+}$-type chromophore, D is ferrocene, and A is a MV^{2+}-type electron acceptor, have been synthesized with the purpose of investigating photo-induced charge separation.[140]

The ground-state absorption properties of the Fc-containing dyads are reported in Table 10, while their electrochemical behavior is shown in Table 11. For the dyads and triads containing the MV^{2+} groups no luminescence was detected at room temperature and at 77 K, indicating that complete quenching ($k_q > 10^9$ s^{-1}) of the excited state of P takes place. It is interesting to notice that the appended ferrocenyl group significantly perturbs the electronic system of the chromophore. Figure 26 compares the absorption spectra of $Ru(ttpy)_2^{2+}$ and of the $(Fc\text{-}phtpy)Ru(ttpy)^{2+}$ dyad. The difference spectrum exhibits a maximum at 510 nm which is likely associated with a CT transition from ferrocene to the π^* ligand orbitals of the photosensitizer (a similar band is present in the Os-containing analogue[140,162]). This interpretation is confirmed by the following results: (i) the Fc-phtpy fragment exhibits an absorption band (λ = 451 nm and ϵ = 1220 M^{-1} cm^{-1} in CH_2Cl_2) which is red-shifted and much more intense

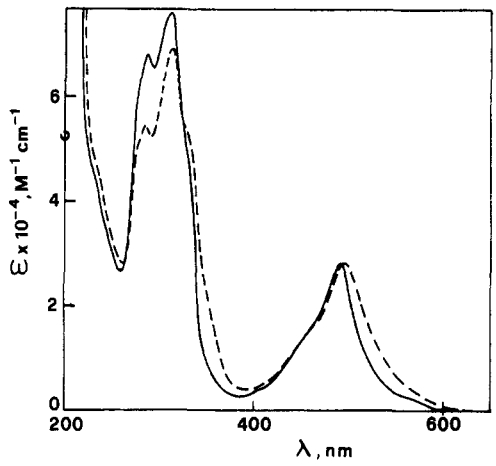

Figure 26. Absorption spectra of $Ru(ttpy)_2^{2+}$ (full line) and (Fc-phtpy)$Ru(ttpy)^{2+}$ (dashed line).

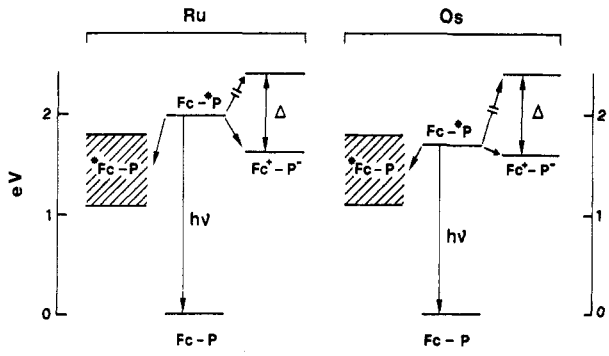

Figure 27. Energy-level diagrams for the Ru- and Os-based Fc–P dyads. For more details, see text.

than that of the ferrocene alone ($\lambda = 442$ nm, $\epsilon = 90$ M^{-1} cm^{-1}); (ii) for the $Zn(Fc\text{-}phtpy)_2^{2+}$ species, where the $Zn(ttpy)_2^{2+}$ unit does not absorb in the visible, this intercomponent band can clearly be observed and is found to be sensitive to the polarity of the solvent (λ_{max} = 491 and 517 nm in CH_3CN and CH_2Cl_2, respectively).[162]

These findings indicate that there is a nonnegligible interaction between the appended ferrocenyl group and the photosensitizer P and suggest that fast intramolecular quenching processes, *via* energy and/or electron transfer, can take place upon formation of *P.

The result of the competition between energy and electron transfer will depend, of course on energetics and nuclear and electronic factors. The diagrams depicted in Figure 27 show the energy level of the states involved in the deactivation of the excited Fc–*P dyads.

For the electron-transfer step, which leads to population of the Fc^+–P^- state, the driving force as obtained from the spectroscopic and electrochemical data (Tables 10 and 11) is −0.34 and −0.1 eV for the Ru- and Os-based system, respectively. The energetics of the energy-transfer step, which involves the ^{3}MLCT state of P as a donor and the triplet of Fc as an acceptor, is difficult to estimate, as there are some uncertainties on the energy level of the latter.[82,130-132] This is because luminescence of the lowest-lying excited state of Fc, which is known to be MC in nature and therefore largely distorted, has never been observed. Estimates for the E^{0-0} of the lowest triplet energy level of ferrocene range between 1.8[132,163] and 1.1[82] eV (Figure 27, dashed areas). The latter value was estimated by employing a general classical treatment to the quenching of the triplet excited state of a family of aromatic molecules by ferrocene.[82] It is likely, therefore, that the triplet level of *Fc is shifted to such low values that the associated emission of light (if any) cannot be detected with a conventional ($\lambda < 900$ nm) luminescence apparatus.[162]

It is apparent from the energy schemes drawn in Figure 27 that at room temperature (i) for the Ru-based dyad both electron and energy-transfer are expected to be energetically allowed and (ii) for the Os-containing dyad energy transfer can be endothermic by ~0.1 eV (if the triplet level is considered to lie at 1.8 eV) or fully exothermic, and electron transfer is slightly exothermic (by ~−0.1 eV).

Experiments on the luminescence properties of both systems at room temperature and at 77 K have revealed that the luminescence quenching is complete in each case.[162] At liquid nitrogen temperature, the employed solvent (butyronitrile) is frozen and the charge separation levels are expected to be destabilized, with respect to what happens at room temperature, by an amount related to the changes in polarity of the solvent on passing from fluid to frozen medium.[164] This is a well-known effect and, for instance, results in no quenching of the luminescence of $*Os(ttpy)_2^{2+}$–MV^{2+} in frozen solvent at 90 K[112] while such quenching is fully effective at room temperature (the room temperature driving force for formation of $Os(ttpy)_2^{3+}$–MV^+ is −0.44 eV, section 12.4.1). According to the Weller treatment,[164] for the cases of the Fc-containing dyads the charge-separated level in rigid matrix should be pushed higher in energy by Δ ~1.5 eV. A value of Δ ~0.8 eV was however experimentally observed for systems[165] in which the donor–acceptor separation is 11 Å, i.e. close to the ferrocene–metal separation of 11.5 Å. If one uses this lower limit for Δ, electron transfer in rigid matrix becomes endothermic by ~0.4 and ~0.7 eV for the Ru- and Os-based dyads, respectively (Figure 27). On the contrary, the energetics of the energy transfer is practically unaffected as the energy levels of the involved excited states are only slightly affected by the rigid medium. In conclusion, for the Ru-containing dyad, energy transfer is expected to be an allowed process, regardless of the "true" position of the triplet of ferrocene and of the working temperature. For the Os-containing dyad, the occurrence of the luminescence quenching at 77 K, that can be safely ascribed to energy transfer as the electron-transfer step is clearly prevented, implies that the energy of the ferrocene triplet is ≤1.69 eV (which is the value of the energy level of the ^{3}MLCT state of $Os(ttpy)_2^{2+}$).

It can be seen that if the "true" energy level of the triplet of ferrocene is ≤1.6 eV the lowest-lying excited state of the Fc–P dyads will be localized on the ferrocene fragment, *Fc–P (the energy of the Fc^+–P^- state is ~1.6–1.7 eV, see Table 11). This would have remarkable consequences because the quenching of the Fc–*P excited state via electron transfer with formation of the Fc^+–P^- charge-separated state would eventually be followed by a (presumably fast) decay to the low-lying *Fc–P excited state. For the Fc–P–MV^{2+} triads a fully charge-separated state is expected to lie at ~1 eV.[162] However its formation should in part compete with formation and radiationless decay of *Fc–P–MV^{2+}.

These arguments suggest that, when designing molecular assemblies in which ferrocene is to be involved as an electron-donor site, the ability of the ferrocene center to play as an energy sink must be carefully taken into account.

13. Conclusions

Bidentate bpy-type and terdentate tpy-type ligands can be used to obtain Ru(II) and Os(II) metal complexes capable of playing the role of photosensitizers in covalently-linked multicomponent systems. Although $M(tpy)_2^{2+}$-type complexes exhibit less favorable photophysical properties (in particular, a short excited-state lifetime at room temperature in the case of M = Ru) compared with $M(bpy)_3^{2+}$, their symmetry properties are much more advantageous. Firstly, $M(tpy)_2^{2+}$ complexes are achiral, contrary to what happens for $M(bpy)_3^{2+}$. Secondly, two substituents on $M(bpy)_3^{2+}$ complexes can give rise to triads with cis-type geometrical arrangements, without possibility of control, whereas substituents in the 4'-positions of $M(tpy)_2^{2+}$ lead to triads where the two substituents lie in opposite directions with respect to the photosensitizer (trans-type arrangement). Derivatives of tpy bearing electron donors or acceptors at the 4'-position can be synthesized and then used to obtain dyad and triad systems where photoinduced charge separation can take place. Rod-like bridging bis-tpy ligands can be obtained by connecting two terpyridine units either directly or through a rigid spacer via the 4'-positions. Such bridging ligands can then be used to coordinate different metals for energy-transfer investigations, or the same metal in two different oxidation states for intervalence transfer studies. The results so far obtained show that the strong electronic interaction observed when the two metal ions are separated by a tpy-tpy bridge decreases upon interposition of 1 or 2 phenyl spacers but remains large enough to allow fast energy transfer ($k > 5 \times 10^{10}$ s^{-1} for (ttpy)*Ru(tpy-(ph)$_2$-tpy)Os(ttpy)$^{4+}$)[104] and relatively intense ($\epsilon = 710\ M^{-1}\ cm^{-1}$ for (ttpy)Ru^{II}(tpy-(ph)$_2$-tpy)Ru^{III}(ttpy)$^{5+}$) intervalence transfer bands.[148] The rate of the photoinduced charge-separation process in the $M(tpy)_2^{2+}$-MV^{2+} dyads is relatively slow because of the small exoergonicity and high intrinsic barrier, whereas the charge recombination reaction is relatively slow presumably because it lies in the Marcus inverted region. The charge recombination reaction in the fully charge-separated state of the triads is relatively fast. Interpretation of the rate constants of the electron-transfer processes in the light of current theories is not easy because the partially covalent character of the M–tpy bond and the electronic interactions between the tpy ligands and the appended donor/acceptor groups do not permit one to know exactly the amount and location of the transferred electronic charge in the various steps. Finally, it can be shown that Fc, contrary to what is generally thought, is not an ideal electron-donor component in photoexcited supramolecular systems because of the presence of a low-lying MC excited state which can play the role of intermediate in fast radiationless processes.

14. Abbreviations

py	pyridine
bpy	2,2'-bipyridine
tpy	2,2':6',2''-terpyridine
Cl-tpy	4'-chloro-2,2':6',2''-terpyridine
Me_2N-tpy	4'-(dimethylamino)-2,2':6',2''-terpyridine
HO-tpy	4'-hydroxy-2,2':6',2''-terpyridine
$MeSO_2$-tpy	4'-(dimethylsulfonyl)-2,2':6',2''-terpyridine
EtO-tpy	4'-ethoxy-2,2':6',2''-terpyridine
ph-tpy	4'-phenyl-2,2':6',2''-terpyridine
Cl-phtpy	4'-(*p*-chlorophenyl)-2,2':6',2''-terpyridine
Br-phtpy	4'-(*p*-bromophenyl)-2,2':6',2''-terpyridine
ttpy	4'-(*p*-tolyl)-2,2':6',2''-terpyridine
HO-phtpy	4'-(*p*-hydroxyphenyl)-2,2':6',2''-terpyridine
MeO-phtpy	4'-(*p*-methoxyphenyl)-2,2':6',2''-terpyridine
4,4'-dptpy	4,4'-diphenyl-2,2':6',2''-terpyridine
6,6''-dptpy	6,6''-diphenyl-2,2':6',2''-terpyridine
tphtpy	4,4',4''-triphenyl-2,2':6',2''-terpyridine
tppz	2,3,5,6-tetrakis(2-pyridyl)pyrazine
phbp-H	6-phenyl-2,2'-bipyridine
dpb-H	di(*o*-pyridyl)-1,3-benzene
tpbp-H_2	3,3',5,5'-tetrapyridylbiphenyl
MePTZ	10-methylphenothiazine
MV^{2+}	1,1'-dimethyl-4,4'-bipyridinium
MeDPAA	methyldi(*p*-anisyl)amine

For other compounds, Fc-phtpy, PTZ-ttpy, DPAA-phtpy, ttpy-MV^{2+}, tpy-tpy, tpy-ph-tpy, and tpy-(ph)$_2$-tpy, see Figures 12–14.

The strucutre formula of the $M(tpy)_2^{2+}$ complexes discussed in this paper is the following:

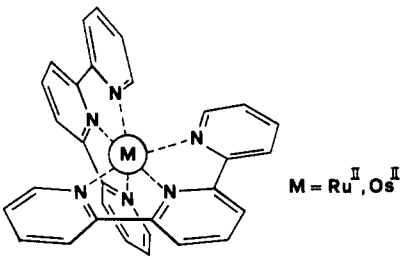

Acknowledgments. This work was supported by the Centre National de la Recherche Scientifique and Ministère de la Recherche (France), and by the Consiglio Nazionale delle Ricerche e Ministero della Università e Ricerca Scientifica e Tecnologica (Italy). A NATO grant (no. 920446, Supramolecular Chemistry) is also acknowledged.

References

(1) Hautala, R. R.; King, R. B.; Kutal C. In *Solar Energy Chemical Conversion and Storage*; Hautala, R. R., King, R. B., Kutal R., Eds.; Humana Press: Clifton, NJ, 1979; p 333.
(2) Dürr, H., Bouas-Laurent, H., Eds. *Photochromism, Molecules and Systems*; Elsevier: The Netherlands, 1990.
(3) Lehn, J.-M. *Angew. Chem., Int. Ed. Engl.* **1988**, *27*, 89.
(4) Ringsdorf, H.; Schlarb, B.; Venzmer, J. *Angew. Chem., Int. Ed. Engl.* **1988**, *27*, 113.
(5) Lehn, J.-M. *Angew Chem., Int. Ed. Engl.* **1990**, *29*, 1304.
(6) Vögtle, F. *Supramolecular Chemistry*; Wiley: Chichester, U.K., 1991.
(7) Balzani, V.; Scandola, F. *Supramolecular Photochemistry*; Horwood: Chichester, U. K., 1991.
(8) Schneider, J., Dürr, H., Eds. *Frontiers in Supramolecular Organic Chemistry and Photochemistry*; VCH Weinheim, Germany, 1991.
(9) Balzani, V., De Cola, L., Eds. *Supramolecular Chemistry*; Kluwer: Dordrecht, Holland, 1992.
(10) Balzani, V. *Tetrahedron*, **1992**, *48*, 10443.
(11) The most authoritative and widely accepted definition of *supramolecular chemistry* is "the chemistry beyond the molecule, bearing on the organized entities of higher complexity that result from the association of two or more chemical species held together by intermolecular forces".[3] Species made of weakly interacting covalently-linked components which retain at least in part their identity, as if they were bound together in a noncovalent fashion, can be taken as belonging to the supramolecular domain.[12] This

approach is very convenient in photochemistry, photophysics, and electrochemistry, as it will be discussed in section 3.[7]
(12) Lehn, J.-M. In *Organic Chemistry: Its Language and Its State of the Art*; Kisakürek, M. V., Ed.; VCH; Basel, 1993; p 77.
(13) Balzani, V., Moggi, L.; Scandola, F. In *Supramolecular Photochemistry*; Balzani, V., Ed.; Reidel: Dordrecht, The Netherlands, 1987; p 1.
(14) (a) Denti, G.; Campagna, S.; Serroni, S.; Ciano, M.; Balzani, V. *J. Am. Chem. Soc.* **1992**, *114*, 2944. (b) Denti, G.; Campagna, S.; Balzani, V. In *Mesomolecules: from Molcules to Materials*; Mendenhall, D., Greensberg, A., Leibman, J., Eds.; Chapman and Hall; New York, in press.
(15) Fox, M. A.; Jones, W. E., Jr.; Watkins, D. M. *Chem. Eng. News* **1993**, *71* (March 15), 38.
(16) Nowakowska, M.; Foyle, V. P.; Guillet, J. E. *J. Am. Chem. Soc.* **1993**, *115*, 5975.
(17) Gust, D.; Moore, T. A.; Moore, A. L. *Acc. Chem. Res.* **1993**, *26*, 198.
(18) Wasielewski, M. R. *Chem. Rev.* **1992**, *92*, 435.
(19) Connolly, J. S.; Bolton, J. R. In *Photoinduced Electron Transfer*; Fox, M. A., Channon, M. Eds.; Elsevier: Amsterdam, 1988; Part D, p 303.
(20) (a) O'Regan, B.; Grätzel, M. *Nature* **1991**, *353*, 738. (b) Nazeeruddin, M. K.; Kay, A.; Rodicio, I.; Humphry-Baker, R.; Müller, E.; Liska, P.; Vlachopoulos, N.; Grätzel, M. *J. Am. Chem. Soc.* **1993**, *115*, 6382.
(21) (a) Hopfield, J. J.; Onuchic, J. N.; Beratan, D. N. *J. Phys. Chem.* **1989**, *93*, 6350. (b) Lloyd, S. *Science* **1993**, *261*, 1569.
(22) Hader, D. P.; Tevini, M. *General Photobiology*; Pergamon: Elmsford, NY, 1987.
(23) Breton, J.; Vermeglio, H., Eds. *The Photosynthetic Bacterial Reaction Center. Structure and Dynamics*; Plenum: New York, 1988.
(24) Deisenhofer, J.; Michel, H. *Angew. Chem., Int. Ed. Engl.* **1989**, *28*, 829.
(25) Huber, R. *Angew. Chem., Int. Ed. Engl.* **1989**, *28*, 848.
(26) Boxer, S. G.; Goldstein, R. A.; Lockhart, D. J.; Middendorf, T. R.; Takiff, L. *J. Phys. Chem.* **1989**, *93*, 8280.
(27) Friesner, R. A.; Won, Y. *Photochem. Photobiol.* **1989**, *50*, 83.
(28) Feher, G.; Allen, J. P.; Okamura, M. Y.; Rees, D. C. *Nature* **1989**, *111*.
(29) Moser, C. C.; Keske, J. M.; Warncke, K.; Farid, M. S.; Duttin, P. L. *Nature* **1992**, *355*, 796.
(30) Deisenhofer, J.; Epp, O.; Miki, K.; Huber, R.; Michel, H. *J. Mol. Biol.* **1984**, *184*, 385.
(31) Bixon, M.; Jortner, J.; Michel-Beyerle, M. E.; Orgodnik, A.; Lersch, W. *Chem. Phys. Lett.* **1987**, *140*, 626.
(32) Marcus, R. A. *Chem. Phys. Lett.* **1987**, *133*, 471.
(33) Fleming, G. R.; Martin, J. L.; Breton, J. *Nature* **1988**, *333*, 190.
(34) Moser, C. C.; Alegria, G.; Gunner, M. R.; Dutton, P. L. In *Photochemical Energy Conversion*; Norris, J. R., Jr., Meisel, D., Eds.; Elsevier: Amsterdam, 1989; p 221.
(35) Holzapfel, W.; Finkele, U.; Kaiser, W.; Oesterhelt, D.; Scheer, H.; Stilz, H. U.; Zinth, W. *Chem. Phys. Lett.* **1989**, *160*, 1.
(36) Franzen, S.; Goldstein, R. F.; Boxer, S. G. *J. Phys. Chem.* **1993**, *97*, 3040.
(37) Hammerstod-Pedersen, J. M.; Jensen, M. H.; Kharkats, Y. I.; Kuznetsov, A. M.; Ulstrup, J. *Chem. Phys. Lett.* **1993**, *205*, 591.
(38) Marchi, M.; Gehlen, J. N.; Chandler, D.; Newton, M. *J. Am. Chem. Soc.* **1993**, *115*, 4178.
(39) Kirmaier, C.; Holten, D.; Parson, W. W. *Biochim. Biophys. Acta* **1985**, *810*, 33.
(40) Holten, D.; Windsor, M. W.; Parson, W. W.; Thornber, J. P. *Biochim. Biophys. Acta* **1978**, *501*, 112.
(41) Dutton, P. L.; Leigh, J. S.; Prince, R. C.; Tiede, D. M. In *Tunneling in Biological Systems*; Chance, B., DeVault, D. C., Frauenfelder, H., Marcus, R. A., Schrieffer, J. R., Sutin, N., Eds.; Academic: New York, 1979; p 319.
(42) Dietrich-Buchecker, C. O.; Sauvage, J.-P. *Chem. Rev.* **1987**, *87*, 795.
(43) Lehn, J.-M.; Rigault, A.; Siegel, J.; Harrowfield, J.; Chevrier, B.; Moras, D. *Proc. Natl. Acad. Sci. U.S.A.* **1987**, *84*, 2565.
(44) Dietrich-Buchecker, C. O.; Sauvage, J.-P. *Angew. Chem., Int. Ed. Engl.* **1989**, *28*, 189.
(45) Constable, E. C.; Ward, M. D. *J. Am. Chem. Soc.*, **1990**, *112*, 1256.
(46) Sauvage, J.-P. *Acc. Chem. Res.* **1990**, *23*, 319.
(47) Williams, A. F.; Piguet, C.; Bernardinelli, G. *Angew. Chem., Int. Ed. Engl.* **1991**, *30*, 1490.
(48) Whitesides, G.; Mathias, J. P.; Seto, C. T. *Science* **1991**, *254*, 1321.
(49) Lindsey, J. S. *New. J. Chem.* **1991**, *15*, 153.
(50) Lehn, J.-M. In *Perspectives in Coordination Chemistry*; Williams, A. F., Floriani, C., Merbach, A. E., Eds.; Verlag Helvetica Chimica Acta: Basel and VCH, Weinheim, 1992; p 447.
(51) Anelli, P. L.; Ashton, P. R.; Ballardini, R.; Balzani, V.; Gandolfi, M. T.; Goodnow, T. T.; Kaifer, A. E.; Pietraskiewicz, M.; Prodi, L.; Reddington, M. V.; Slawin, A. M. Z.; Spencer, N.; Stoddart, J. F.; Vicent, C.; Williams, D. J. *J. Am. Chem. Soc.* **1992**, *114*, 193.
(52) Baxter, P.; Lehn, J.-M.; DeCian, A.; Fischer, J. *Angew. Chem., Int. Ed. Engl.* **1993**, *32*, 69.
(53) Bush, D. H. *Chem. Rev.* **1993**, *93*, 847.
(54) (a) Newkome, G. R.; Yao, Z.-q.; Baker, G. R.; Gupta, V. K.; Russo, P. S.; Saunders, M. J. *J. Am. Chem. Soc.* **1986**, *108*, 849. (b) Newkome, G. R.; Cardullo, F.; Constable, E. C.; Moorefield, C. N.; Cargill Thompson, A. M. W. *J. Chem. Soc., Chem. Commun*, **1993**, 925.
(55) (a) Hawker, C. J.; Fréchet, J. M. J. *J. Am. Chem. Soc.* **1990**, *112*, 7638. (b) Lochmann, L.; Wooley, K. L.; Ivanova, P. T.; Fréchèt, J. M. J. *J. Am. Chem. Soc.* **1993**, *115*, 7043.
(56) (a) Tomalia, D. A.; Naylor, A. M.; Goddard, W. A. III. *Angew. Chem., Int. Ed. Engl.* **1990**, *29*, 138. (b) Tomalia, D. A.; Durst, H. D. *Top. Curr. Chem.* **1993**, *165*, 193.
(57) Serroni, S.; Denti, G.; Campagna, S.; Juris, A.; Ciano, M.; Balzani, V. *Angew. Chem., Int. Ed. Engl.* **1992**, *31*, 1495.
(58) Kaszynski, P.; Friedli, A. C.; Michl, J. *J. Am. Chem. Soc.* **1992**, *114*, 601.
(59) Xu, Z.; Moore, J. S. *Angew. Chem., Int. Ed. Engl.* **1993**, *32*, 1354.
(60) Marcus, R. A. *Annu. Rev. Phys. Chem.* **1964**, *15*, 155.
(61) Sutin, N. *Prog. Inorg. Chem.* **1983**, *30*, 441.
(62) Marcus, R. A.; Sutin, N. *Biochim. Biophys. Acta* **1985**, *811*, 265 and refs. therein.
(63) Sutton, J. E.; Taube, H. *Inorg. Chem.* **1981**, *20*, 3125 and refs. therein.
(64) Mulliken, R. S.; Person, W. B. *Molecular Complexes*; Wiley: New York, 1969.
(65) De la Rosa, R.; Chang, P. Y.; Salaymeth, F.; Curtis, J. C. *Inorg. Chem.* 1385, *24*, 4229.
(66) (a) Mines, G. A.; Roberts, J. A.; Hupp, J. T. *Inorg. Chem.* **1992**, *31*, 125. (b) Dong, Y.; Hupp, J. T. *Inorg. Chem.* **1992**, *31*, 3170. (c) Hupp, J. T.; Dong, Y.; Blackbourn, R. L.; Lu, H. *J. Phys. Chem.* **1993**, *97*, 3278.
(67) (a) Oh, D. H.; Boxer, S. G. *J. Am. Chem. Soc.* **1990**, *112*, 8161. (b) Oh, D. H.; Sano, M.; Boxer, S. G. *J. Am. Chem. Soc.* **1991**, *113*, 6880.
(68) McConnell, H. M. *J. Chem. Phys.*, **1961**, *35*, 508.
(69) Richardson, D. E.; Taube, H. *J. Am. Chem. Soc.* **1983**, *105*, 40.
(70) Miller, J. R.; Beitz, J. V. *J. Chem. Phys.* **1981**, *74*, 6746.
(71) Wasielewski, M. R. In *Photoinduced electron transfer. Part D*; Fox, M. A., Chanon, M., Eds.; Elsevier: Amsterdam, p 161.
(72) Liang, C.; Newton, M. D. *J. Phys. Chem.* **1993**, *97*, 3199.
(73) Curtiss, L. A.; Naleway, C. A.; Miller, J. R. *J. Phys. Chem.* **1993**, *97*, 4050.
(74) Jortner, J. *J. Chem. Phys.* **1976**, *64*, 4860.
(75) Hush, N. S. *Prog. Inorg. Chem.* **1967**, *8*, 391.
(76) Oevering, H.; Verhoeven, J. W.; Paddon-Row, M. N.; Warman, J. M. *Tetrahedron* **1989**, *45*, 4751.
(77) Gould, I. R.; Noukakis, D.; Gomez-John, L.; Goodman, J. L.; Farid, S. *J. Am. Chem. Soc.* **1993**, *115*, 4405.
(78) Creutz, C. *Prog. Inorg. Chem.* **1980**, *30*, 1.
(79) Robin, M. B.; Day, P. *Adv. Inorg. Chem. Radiochem.* **1967**, *10*, 247.
(80) Förster, Th. H. *Discussion Faraday Soc.* **1959**, *27*, 7.
(81) Dexter, D. L. *J. Chem. Phys.* **1953**, *21*, 836.
(82) Balzani, V.; Bolletta, F.; Scandola, F. *J. Am. Chem. Soc.* **1980**, *102*, 2152.
(83) Scandola, F.; Balzani, V. *J. Chem. Educ.* **1983**, *60*, 814.
(84) Sutin, N. *Acc. Chem. Res.* **1982**, *15*, 275.
(85) Orlandi, G.; Monti, S.; Barigelletti, F.; Balzani, V. *Chem. Phys.* **1980**, *52*, 313.
(86) (a) Balzani, V.; Bolletta, F.; Gandolfi, M. T.; Maestri, M. *Top. Curr. Chem.* **1978**, *75*, 1. (b) Juris, A.; Balzani, V.; Barigelletti, F.; Campagna, S.; Belser, P.; von Zelewsky, A. *Coord. Chem. Rev.* **1988**, *84*, 85. (c) Meyer, T. J. *Pure Appl. Chem.* **1986**, *58*, 1193.
(87) (a) Balzani, V.; Barigelletti, F.; De Cola, L. *Top. Curr. Chem.* **1990**, *158*, 31. (b) Balzani, V.; Maestri, M. In *Photosensitization and Photocalysis Using Inorganic and Organometallic Compounds*; Kalyanasundaram, K., Grätzel, M., Eds.; Kluwer: Dordrecht, The Netherlands, 1993; p 15.
(88) Stone, M. L.; Crosby, G. A. *Chem. Phys. Lett.* **1981**, *79*, 169.
(89) Lin, C.-I.; Bottcher, W.; Chou, M.; Creutz, C.; Sutin, N. *J. Am. Chem. Soc.* **1976**, *98*, 6536.
(90) Young, R. C.; Nagle, J. K.; Meyer, T. J.; Whitten, D. G. *J. Am. Chem. Soc.* **1978**, *100*, 4773.
(91) Kirchhoff, J. R.; McMillin, D. R.; Marnot, P. A.; Sauvage, J. P. *J. Am. Chem. Soc.* **1985**, *107*, 1138.
(92) Hacker, C. R.; Gushurst, A. K. I.; McMillin, D. R. *Inorg. Chem.* **1991**, *30*, 538.
(93) Creutz, C.; Chou, M.; Netzel, T. L.; Okumura, M.; Sutin, N. *J. Am. Chem. Soc.* **1980**, *102*, 1309.
(94) Winkler, J. R.; Netzel, T. L.; Creutz, C.; Sutin, N. *J. Am. Chem. Soc.* **1987**, *109*, 2381.
(95) Fink, D. W.; Ohnesorge, W. E. *J. Am. Chem. Soc.* **1969**, *91*, 4995.
(96) Lytle, F. E.; Petrosky, L. M.; Carlson, L. R. *Anal. Chim. Acta* **1971**, *57*, 239.
(97) Calvert, J. M.; Caspar, J. V.; Binstead, R. A.; Westmoreland, T. D.; Meyer, T. J. *J. Am. Chem. Soc.* **1982**, *104*, 6620.
(98) Bessel, C. A.; See, R. F.; Jameson, D. L.; Churchill, M. R.; Takeuchi, K. J. *J. Chem. Soc., Dalton Trans.* **1992**, 3223.
(99) Constable, E. C.; Cargill Thompson, A. M. W.; Tocher, D. A.; Daniels, M. A. M. *New. J. Chem.* **1992**, *16*, 855.
(100) Hecker, C. R.; Fanwick, P. E.; McMillin, D. *Inorg. Chem.* **1991**, *30*, 659.

(101) Amouyal, E.; Mouallem-Bahout, M.; Calzaferri, G. *J. Phys. Chem.* **1991**, *95*, 7641.
(102) Beley, M.; Collin, J.-P.; Sauvage, J.-P.; Sugihara, H.; Heisel, F.; Miehé, A. *J. Chem. Soc., Dalton Trans.* **1991**, 3157.
(103) Constable, E. C.; Cargill Thompson, A. M. W.; Armaroli, N.; Balzani, V.; Maestri, M. *Polyhedron* **1992**, *20*, 2707.
(104) Constable, E. C.; Cargill Thompson, A. M. W.; Armaroli, N.; Balzani, V.; Maestri, M. To be published.
(105) Barigelletti, F.; Flamigni, L.; Balzani, V.; Collin, J.-P.; Sauvage, J.-P.; Sour, A.; Constable, E. C.; Cargill-Thompson, A. M. W. *J. Chem. Soc., Chem. Commun.* **1993**, 942.
(106) Collin, J.-P.; Guillerez, S.; Sauvage, J.-P.; Barigelletti, F.; Flamigni, L.; De Cola, L.; Balzani, V. *Coord. Chem. Rev.* **1991**, *111*, 291.
(107) Collin, J.-P.; Guillerez, S.; Sauvage, J.-P.; Barigelletti, F.; De Cola, L.; Flamigni, L.; Balzani, V. *Inorg. Chem.* **1991**, *30*, 4230.
(108) Arana, C. R.; Abruña, H. D. *Inorg. Chem.* **1993**, *32*, 194.
(109) Petersen, J. D. In *Supramolecular Photochemistry*; Balzani, V., Ed.; Reidel: Dordrecht, The Netherlands, 1987; p 135.
(110) Demas, J. N.; Crosby, G. A. *J. Am. Chem. Soc.* **1971**, *93*, 2841.
(111) Kober, E. M.; Marshall, J. L.; Dressick, W. J.; Sullivan, B. P.; Caspar, J.-V.; Meyer, T. J. *Inorg. Chem.* **1985**, *24*, 2755.
(112) Collin, J.-P.; Guillerez, S.; Sauvage, J.-P.; Barigelletti, F.; De Cola, L.; Flamigni, L.; Balzani, V. *Inorg Chem.* **1992**, *31*, 4112.
(113) Collin, J.-P.; Beley, M.; Sauvage, J.-P.; Barigelletti, F. *Inorg. Chim. Acta* **1991**, *186*, 91.
(114) Beley, M.; Chodorowsky, S.; Collin, J.-P.; Sauvage, J.-P.; Flamigni, L.; Barigelletti, F. *Inorg. Chem.*, in press.
(115) Phifer, C. C.; McMillin, D. R. *Inorg. Chem.* **1986**, *25*, 1329.
(116) Liu, D. K.; Brunschwig, B. S.; Creutz, C.; Sutin, N. *J. Am. Chem. Soc.* **1986**, *108*, 1749.
(117) Brunschwig, B. S.; Sutin, N. *J. Am. Chem. Soc.* **1978**, *100*, 7568.
(118) Ayala, N. P.; Flynn, C. M.; Sacksteder, L. A.; Demas, J. N.; De Graff, B. A. *J. Am. Chem. Soc.* **1990**, *112*, 3837.
(119) Ohno, T.; Kato, S.; Kaiazaki, S.; Hanazaki, I. *Inorg. Chem.* **1986**, *25*, 3853.
(120) Kalyanasundaram, K. *Photochemistry of Polypyridine and Porphyrin Complexes*; Academic Press: New York, 1992.
(121) Vögtle, F.; Frank, M.; Nieger, M.; Belser, P.; von Zelewsky, A.; Balzani, V.; Barigelletti, F.; De Cola, L.; Flamigni, L. *Angew. Chem., Int. Ed. Engl.* **1993**, *32*, 1643.
(122) De Cola, L.; Balzani, V.; Barigelletti, F.; Flamigni, L.; Belser, P.; von Zelewsky, A.; Frank, M.; Vögtle, F. *Inorg. Chem.* **1993**, *32*, 5228.
(123) Constable, E. C.; Cargill-Thompson, A. M. W. *J. Chem. Soc., Dalton Trans.* **1992**, 3467.
(124) Constable, E. C.; Cargill Thompson, A. M. W.; Tôcher, D. A. In *Supramolecular Chemistry*; Balzani, V., De Cola, L., Eds.; Kluwer: Dordrecht, The Netherlands, 1992; p 219.
(125) Danielson, E.; Elliot, C. M.; Merckert, J. W.; Meyer, T. J. *J. Am. Chem. Soc.* **1987**, *109*. 2519.
(126) Constable, E. C. *Adv. Inorg. Chem. Radiochem.* **1986**, *30*, 69.
(127) Collin, J.-P.; Guillerez, S.; Sauvage, J.-P. *J. Chem. Soc., Chem. Commun.* **1989**, 776.
(128) Sauvage, J.-P.; Ward, M. *Inorg. Chem.* **1991**, *30*, 3869.
(129) Warman, J. M.; Smit, K. J.; Jonker, S. A.; Verhoeven, J. W.; Oevering, H.; Kroon, J.; Paddon-Row, M. N.; Oliver, A. M. *Chem. Phys.* **1993**, *170*, 359.
(130) Sohn, Y. S.; Hendrickson, D. N.; Gray, H. B. *J. Am. Chem. Soc.* **1971**, *93*, 3603.
(131) Geoffrey, G. L.; Wrighton, M. S. *Organometallic Photochemistry*; Academic Press: New York, 1979.
(132) (a) Farmilo, A.; Wilkinson, F. *Chem. Phys. Lett.* **1975**, *34*, 575. (b) Herkstroeter, W. G. *J. Am. Chem. Soc.* **1975**, *97*, 4161. (c) Kikuchi, M.; Kikuchi, K.; Kokubun, H. *Bull. Chem. Soc. Jpn.* **1974**, *47*, 1331. (d) Bhattacharyya, K.; Ramaiah, D.; Das, P. K.; George, M. V. *J. Phys. Chem.* **1986**, *90*, 5984.
(133) For recent reviews, see: (a) Scandola, F.; Indelli, M. T.; Chiorboli, C.; Bignozzi, C. A *Top. Curr. Chem.* **1990**, *158*, 73. (b) Schanze, K. S.; MacQueen, D. B.; Perkins, T. A.; Cabana, L. A. *Coord. Chem. Rev.* **1993**, *122*, 63.
(134) Kim, Y.; Lieber, C. M. *Inorg. Chem.* **1989**, *28*, 3990.
(135) (a) Grosshenny, V.; Ziessel, R. *Tetrahedron Lett.* **1992**, *33*, 8075. (b) Grosshenny, V.; Ziessel, R. *J. Chem. Soc., Dalton Trans.* **1993**, 817. (c) Grosshenny, V.; Ziessel, R. *J. Organomet. Chem.* **1993**, *453*, C19.
(136) Case, F. H.; Kasper, T. J. *J. Am. Chem. Soc.* **1956**, *78*, 5842.
(137) Kröhnke, F. *Synthesis* **1976**, 1.
(138) (a) Potts, K. T.; Cipullo, M. J.; Ralli, P.; Theodoridis, G. *J. Org. Chem.* **1982**, *47*, 3027. (b) Jameson, D. L.; Guise, L. E. *Tetrahedron Lett.* **1991**, *32*, 1999.
(139) Spahni, W.; Calzaferri, G. *Helv. Chim. Acta* **1984**, *67*, 450.
(140) (a) Chambron, J.-C.; Coudret, C.; Sauvage, J.-P. *New J. Chem.* **1992**, *16*, 361. (b) Coudret, C. Thesis, Louis Pasteur University, Strasbourg, 1991.
(141) Goodwin, H. A.; Lions, F. *J. Am. Chem. Soc.* **1959**, *81*, 6415.
(142) Constable, E. C.; Ward, M. D. *J. Chem. Soc., Dalton Trans.* **1990**, 1405.
(143) Constable, E. C.; Lewis, J. *Polyhedron* **1982**, *1*, 303.
(144) Collin, J.-P.; Guillerez, S.; Sauvage, J.-P. *Inorg. Chem.* **1990**, *29*, 5009.
(145) Beley, M.; Collin, J.-P.; Louis, R.; Metz, B.; Sauvage, J.-P. *J. Am. Chem. Soc.* **1991**, *113*, 8251.
(146) Thummel, R. P.; Chirayil, S. *Inorg. Chim. Acta* **1988**, *154*, 77.
(147) Collin, J.-P.; Sour, A. Unpublished results.
(148) Collin, J.-P.; Lainé, P.; Launay, J.-P.; Sour, A. *J. Chem. Soc., Chem. Commun.* **1993**, 434.
(149) Vogler, L. M.; Scott, B.; Brewer, K. J. *Inorg. Chem.* **1993**, *32*, 898.
(150) Howard, C. A.; Ward, M. D., *Angew. Chem., Int. Ed. Engl.* **1992**, *31*, 1028.
(151) Woitellier, S.; Launay, J. P.; Spangler, C. W. *Inorg. Chem.* **1988**, *28*, 758.
(152) Beley, M.; Collin, J. P.; Louis, R.; Metz, B.; Sauvage, J.-P. *J. Am. Chem. Soc.* **1991**, *113*, 8521.
(153) Beley, M.; Collin, J.-P.; Sauvage, J.-P. *Inorg. Chem.* **1993**, *32*, 4539.
(154) Amouyal, E.; Mouallem-Bahout, M. *J. Chem. Soc., Dalton Trans* **1992**, 509.
(155) Watanabe, T.; Honda, K. *J. Phys. Chem.* **1982**, *86*, 2613.
(156) Thummel, R. P.; Hedge, V.; Jahng, Y. *Inorg. Chem.* **1989**, *28*, 3264.
(157) Venturi, M.; Mulazzani, Q. G.; Hoffman, M. Z. *Radiat. Phys. Chem.* **1984**, *23*, 229.
(158) Collin, J.-P.; Guillerez, S.; Sauvage, J.-P.; Barigelletti, F.; De Cola, L.; Flamigni, L.; Balzani, V. Unpublished results.
(159) Connolly, J. S.; Bolton, J. R. In *Photoinduced Electron Transfer, Part D*; Fox, M. A., Chanon, M., Eds.; Elsevier: Amsterdam, 1988; p 303.
(160) Berger, R. M.; McMillin, D. R. *Inorg. Chem.* **1988**, *27*, 4245.
(161) (a) Butler, I. R.; Roustan, J.-L. *Can. J. Chem.* **1990**, *68*, 2212. (b) Butler, I. R. *Organometallics* **1992**, *11*, 74. (c) Butler, I. R.; Burke, N.; Hobson, L. J.; Findenegg, H. *Polyhedron* **1992**, *19*, 2435.
(162) De Cola, L.; Flamigni, L.; Barigelletti, F.; Chambron, J.-C.; Coudret, C.; Collin, J.-P.; Sauvage, J. P. Work in progress.
(163) Lee, E. J.; Wrighton, M. K. *J. Am. Chem. Soc.* **1991**, *113*, 8562.
(164) Weller, A. *Z. Phys. Chem. NF* **1982**, *133*, 93.
(165) Gaines, L.; O'Neil, M. P.; Svec, W. A.; Niemczyk, M. P.; Wasielewski, M. R. *J. Am. Chem. Soc.* **1991**, *113*, 719.